



Top-squark searches at the Tevatron in models of low-energy supersymmetry breaking

Marcela Carena^a, Debajyoti Choudhury^b, Rodolfo A. Diaz^c,
Heather E. Logan^a and Carlos E.M. Wagner^{d,e} *

^a *Theoretical Physics Department, Fermilab, PO Box 500, Batavia, Illinois 60510-0500, USA*

^b *Harish-Chandra Research Institute, Chhatnag Road, Jhusi, Allahabad 211 019, India*

^c *Departamento de Fisica, Universidad Nacional de Colombia, Bogota, Colombia*

^d *HEP Division, Argonne National Lab, 9700 S. Cass Ave, Argonne, Illinois 60439, USA*

^e *Enrico Fermi Institute, University of Chicago, 5640 Ellis Ave, Chicago, Illinois 60637, USA*

Abstract

We study the production and decays of top squarks (stops) at the Tevatron collider in models of low-energy supersymmetry breaking. We consider the case where the lightest Standard Model (SM) superpartner is a light neutralino that predominantly decays into a photon and a light gravitino. Considering the lighter stop to be the next-to-lightest Standard Model superpartner, we analyze stop signatures associated with jets, photons and missing energy, which lead to signals naturally larger than the associated SM backgrounds. We consider both 2-body and 3-body decays of the top squarks and show that the reach of the Tevatron can be significantly larger than that expected within the standard supergravity models. For a modest projection of the final Tevatron luminosity, $\mathcal{L} \simeq 4 \text{ fb}^{-1}$, stop masses of order 300 GeV are accessible at the Tevatron collider in both 2-body and 3-body decay modes. We also consider the production and decay of ten degenerate squarks that are the supersymmetric partners of the five light quarks. In this case we find that common squark masses up to 360 GeV are easily accessible at the Tevatron collider, and that the reach increases further if the gluino is light.

*Electronic addresses: carena@fnal.gov, debchou@mri.ernet.in, radiaz@ciencias.unal.edu.co, logan@fnal.gov, cwagner@hep.anl.gov

1 Introduction

The Standard Model with a light Higgs boson provides a very good description of all experimental data. The consistency of the precision electroweak data with the predictions of the Standard Model suggests that, if new physics is present at the weak scale, it is most probably weakly interacting and consistent with the presence of a light Higgs boson in the spectrum. Extensions of the Standard Model based on softly broken low energy supersymmetry (SUSY) [1] provide the most attractive scenarios of physics beyond the Standard Model fulfilling these properties. If the supersymmetry breaking masses are of the order of 1 TeV, supersymmetry stabilizes the hierarchy between the Planck scale M_P and the electroweak scale. Furthermore, the minimal supersymmetric extension of the Standard Model (MSSM) significantly improves the precision with which the three gauge couplings unify and leads to the presence of a light Higgs boson with a mass below 135 GeV [2].

Perhaps the most intriguing property of supersymmetry is that local supersymmetry naturally leads to the presence of gravity (supergravity). In the case of global supersymmetry, a massless spin one-half particle, the Goldstino, appears in the spectrum when supersymmetry is spontaneously broken. In the case of local supersymmetry, the Goldstino provides the additional degrees of freedom to make the gravitino a massive particle [3]. In the simplest scenarios, the gravitino mass $m_{\tilde{G}}$ is directly proportional to the square of the supersymmetry breaking scale $\sqrt{F_{\text{SUSY}}}$:

$$m_{\tilde{G}} \simeq F_{\text{SUSY}}/\sqrt{3}M_P. \quad (1.1)$$

The relation between the supersymmetry breaking scale $\sqrt{F_{\text{SUSY}}}$ and the supersymmetry particle masses depends on the specific supersymmetry breaking mechanism. In general, the superpartner masses M_{SUSY} are directly proportional to F_{SUSY} and inversely proportional to the messenger scale M_m at which the supersymmetry breaking is communicated to the visible sector:

$$M_{\text{SUSY}} \simeq \alpha \frac{F_{\text{SUSY}}}{M_m}, \quad (1.2)$$

where α is the characteristic coupling constant coupling the messenger sector to the visible one. If the breakdown of supersymmetry is related to gravity effects, M_m is naturally of the order of the Planck scale and α is of order one, so that M_{SUSY} is at the TeV scale if $\sqrt{F_{\text{SUSY}}} \sim 10^{11}$ GeV. In gauge mediated scenarios (GMSB) [4,5], instead, the couplings α are associated with the Standard Model gauge couplings times a loop suppression factor, so that values of F_{SUSY}/M_m of order 100 TeV yield masses for the lighter Standard Model superpartners of order 100 GeV.

When relevant at low energies, the gravitino interactions with matter are well described through the interactions of its spin 1/2 Goldstino component [3]. The Goldstino has derivative couplings with the visible sector with a strength proportional to $1/F_{\text{SUSY}}$. In scenarios with a high messenger scale, of order M_P , Eqs. 1.1 and 1.2 imply that the gravitino has a mass of the same order as the other SUSY particles,

and its interactions are extremely weak. In such scenarios, the gravitino plays no role in the low-energy phenomenology. However, in low energy supersymmetry breaking scenarios such as GMSB in which the messenger scale is significantly lower than the Planck scale, the supersymmetry breaking scale is much smaller. Typical values in the GMSB case are $M_m \sim 10^5 - 10^8$ GeV, leading to a supersymmetry breaking scale $\sqrt{F_{\text{SUSY}}}$ roughly between 10^5 and a few times 10^6 GeV. The gravitino then becomes significantly lighter than the superpartners of the quarks, leptons and gauge bosons, and its interaction strength is larger. As the lightest supersymmetric particle (LSP), the gravitino must ultimately be produced at the end of all superparticle decay chains if R -parity is conserved (for an analysis of the case of R -parity violation see Ref. [6]).

Depending on the strength of the gravitino coupling, the decay length of the next-to-lightest supersymmetric particle (NLSP) can be large (so that the NLSP is effectively stable from the point of view of collider phenomenology; this occurs when $\sqrt{F_{\text{SUSY}}} \gtrsim 1000$ TeV), intermediate (so that the NLSP decays within the detector giving rise to spectacular displaced vertex signals; this occurs when $1000 \text{ TeV} \gtrsim \sqrt{F_{\text{SUSY}}} \gtrsim 100$ TeV), or microscopic (so that the NLSP decays promptly; this occurs when $\sqrt{F_{\text{SUSY}}} \lesssim 100$ TeV) [7–9]. The decay branching fractions of the Standard Model superpartners other than the NLSP into the gravitino are typically negligible. However, if the supersymmetry breaking scale is very low, $\sqrt{F_{\text{SUSY}}} \ll 100$ TeV (corresponding to a gravitino mass $\ll 1$ eV), then the gravitino coupling strength can become large enough that superpartners other than the NLSP may decay directly into final states containing a gravitino [9, 10]. In any case, the SUSY-breaking scale must be larger than the mass of the heaviest superparticle; an approximate lower bound of $\sqrt{F_{\text{SUSY}}} \simeq 1$ TeV yields a gravitino mass of about 10^{-3} eV.

In many models, the lightest supersymmetric partner of a Standard Model particle is a neutralino, $\tilde{\chi}_1^0$. The decay widths of the $\tilde{\chi}_1^0$ into various final state particles are given by:

$$\Gamma(\tilde{\chi}_1^0 \rightarrow X\tilde{G}) \simeq K_X N_X \frac{m_{\tilde{\chi}_1^0}}{96\pi} \left(\frac{m_{\tilde{\chi}_1^0}}{\sqrt{M_P m_{\tilde{G}}}} \right)^4 \left(1 - \frac{m_X^2}{m_{\tilde{\chi}_1^0}^2} \right)^4, \quad (1.3)$$

where K_X is a projection factor equal to the square of the component in the NLSP of the superpartner of the particle X , and N_X is the number of degrees of freedom of X . If X is a photon, for instance, $N_X = 2$ and

$$K_X = |N_{11} \cos \theta_W + N_{12} \sin \theta_W|^2, \quad (1.4)$$

where N_{ij} is the mixing matrix connecting the neutralino mass eigenstates to the weak eigenstates in the basis $\tilde{B}, \tilde{W}, \tilde{H}_1, \tilde{H}_2$.

If the neutralino has a significant photino component, it will lead to observable decays into photon and gravitino. Since the heavier supersymmetric particles decay into the NLSP, which subsequently decays into photon and gravitino, supersymmetric particle production will be characterized by events containing photons and missing energy. This is in contrast to supergravity scenarios, where, unless very specific

conditions are fulfilled [11, 12], photons do not represent a characteristic signature. The presence of two energetic photons plus missing transverse energy provides a distinctive SUSY signature with very little Standard Model background.

If $\tilde{\chi}_1^0$ decays with a large branching ratio into photons, its mass is severely constrained by LEP data. However, this bound is model-dependent: there is no tree-level coupling of the γ and Z to two binos or to two neutral winos, but LEP could produce bino or neutral wino pairs through t -channel exchange of selectrons. Since the bino is associated with the smallest of all gauge interactions and, in addition, its mass is more strongly renormalized downward at smaller scales compared to the wino mass, in many models the lightest neutralino has a significant bino component. Therefore, if the NLSP is approximately a pure bino, the bounds on its mass depend strongly on the selectron mass. For selectron masses below 200 GeV, the present bound on such a neutralino is of about 90 GeV [13]. Then, as emphasized before, it will decay via $\tilde{\chi}_1^0 \rightarrow \gamma\tilde{G}$. If $\tilde{\chi}_1^0$ is heavy enough, then the decays $\tilde{\chi}_1^0 \rightarrow Z\tilde{G}$ and $\tilde{\chi}_1^0 \rightarrow h^0\tilde{G}$ are also kinematically allowed; however, the decay widths into these final states are kinematically suppressed compared to the $\gamma\tilde{G}$ final state and will only be important if the photino component of $\tilde{\chi}_1^0$ is small or if $\tilde{\chi}_1^0$ is significantly heavier than Z and h^0 [9].

In most SUSY models it is natural for the lighter top squark, \tilde{t}_1 , to be light compared to the other squarks. In general, due to the large top Yukawa coupling there is a large mixing between the weak eigenstates \tilde{t}_L and \tilde{t}_R , which leads to a large splitting between the two stop mass eigenstates. In addition, even if all squarks have a common mass at the messenger scale, the large top Yukawa coupling typically results in the stop masses being driven (under renormalization group evolution) to smaller values at the weak scale. An extra motivation to consider light third generation squarks comes from the fact that light stops, with masses of about or smaller than the top quark mass, are demanded for the realization of the mechanism of electroweak baryogenesis within the context of the MSSM [14].

In this paper, we examine in detail the production and decay of top squarks at Run II of the Tevatron collider in low-energy SUSY breaking scenarios, by assuming that the NLSP is the lightest neutralino, which decays promptly to $\gamma\tilde{G}$. We also investigate the production and decay of the other squarks, and provide an estimate of the reach of Run II of the Tevatron in the heavy gluino limit. We work in the context of a general SUSY model in which the SUSY particle masses are *not* constrained by the relations predicted in the minimal GMSB models. We assume throughout that the gravitino coupling is strong enough (or, equivalently, that the scale of SUSY breaking is low enough) that the NLSP decays promptly. This implies an upper bound on the supersymmetry breaking scale of a few tens to a few hundred TeV [7–9], depending on the mass of the NLSP. Our analysis can be extended to higher supersymmetry breaking scales for which the NLSP has a finite decay length, although in this case some signal will be lost due to NLSP decays outside the detector. At least 50% of the diphoton signal cross section remains though for NLSP decay lengths $c\tau \lesssim 40$ cm [7]; this corresponds to a supersymmetry breaking scale below a few hundred to about

a thousand TeV, depending on the mass of the NLSP. Moreover, the displaced vertex associated with a finite decay length could be a very good additional discriminator for the signal. Thus, in totality, our choice is certainly not an overly optimistic one.

This paper is organized as follows. In Sec. 2 we review the stop pair production cross section at the Tevatron. In Sec. 3 we summarize previous studies of stop production and decay at Run II of the Tevatron. In Sec. 4 we discuss the SUSY parameter space and the relative partial widths of the various stop decay modes. In Sec. 5 we describe the signal for each of the stop decay modes considered. We describe the backgrounds and the cuts used to separate signal from background in each case, and give signal cross sections after cuts. This gives the reach at Run II. We also note the possibility that stops can be produced in the decays of top quarks. In Sec. 6 we consider 10 degenerate squarks that are the supersymmetric partners of the five light quarks. In Sec. 7 we summarize our conclusions.

2 Top squark production at Tevatron Run II

Top squarks are produced at hadron colliders overwhelmingly via the strong interaction, so that the tree-level cross sections are model independent and depend only on the stop mass. The production modes of the lighter stop, \tilde{t}_1 , at the Tevatron are $q\bar{q} \rightarrow \tilde{t}_1\tilde{t}_1^*$ and $gg \rightarrow \tilde{t}_1\tilde{t}_1^*$. The cross sections for these processes are well known at leading order (LO) [15, 16], and the next-to-leading order (NLO) QCD and SUSY-QCD corrections have been computed [17] and significantly reduce the renormalization scale dependence. The NLO cross section is implemented numerically in PROSPINO [17, 18].

We generate stop events using the LO cross section evaluated at the scale $\mu = m_{\tilde{t}}$, improved by the NLO K-factor ¹ obtained from PROSPINO [17, 18] (see Fig. 1). The K-factor varies between 1 and 1.5 for $m_{\tilde{t}}$ decreasing from 450 to 100 GeV. We use the CTEQ5 parton distribution functions [19]. We assume that the gluino and the other squarks are heavy enough that they do not affect the NLO cross section. This is already the case for gluino and squark masses above about 200 GeV [17].

Top squarks can also be produced via cascade decays of heavier supersymmetric particles, with a highly model dependent rate. To be conservative, we assume that the masses of the heavier supersymmetric particles are large enough that their production rate at Tevatron energies can be neglected.

3 Previous studies of stops at Run II

A number of previous studies have considered the prospects for stop discovery at Run II of the Tevatron, which we summarize here. In general, the most detailed SUSY studies have been done in the context of

¹Although gluon radiation at NLO leads to a small shift in the stop p_T distribution to lower p_T values [17, 18], we do not expect this shift to affect our analysis in any significant way.

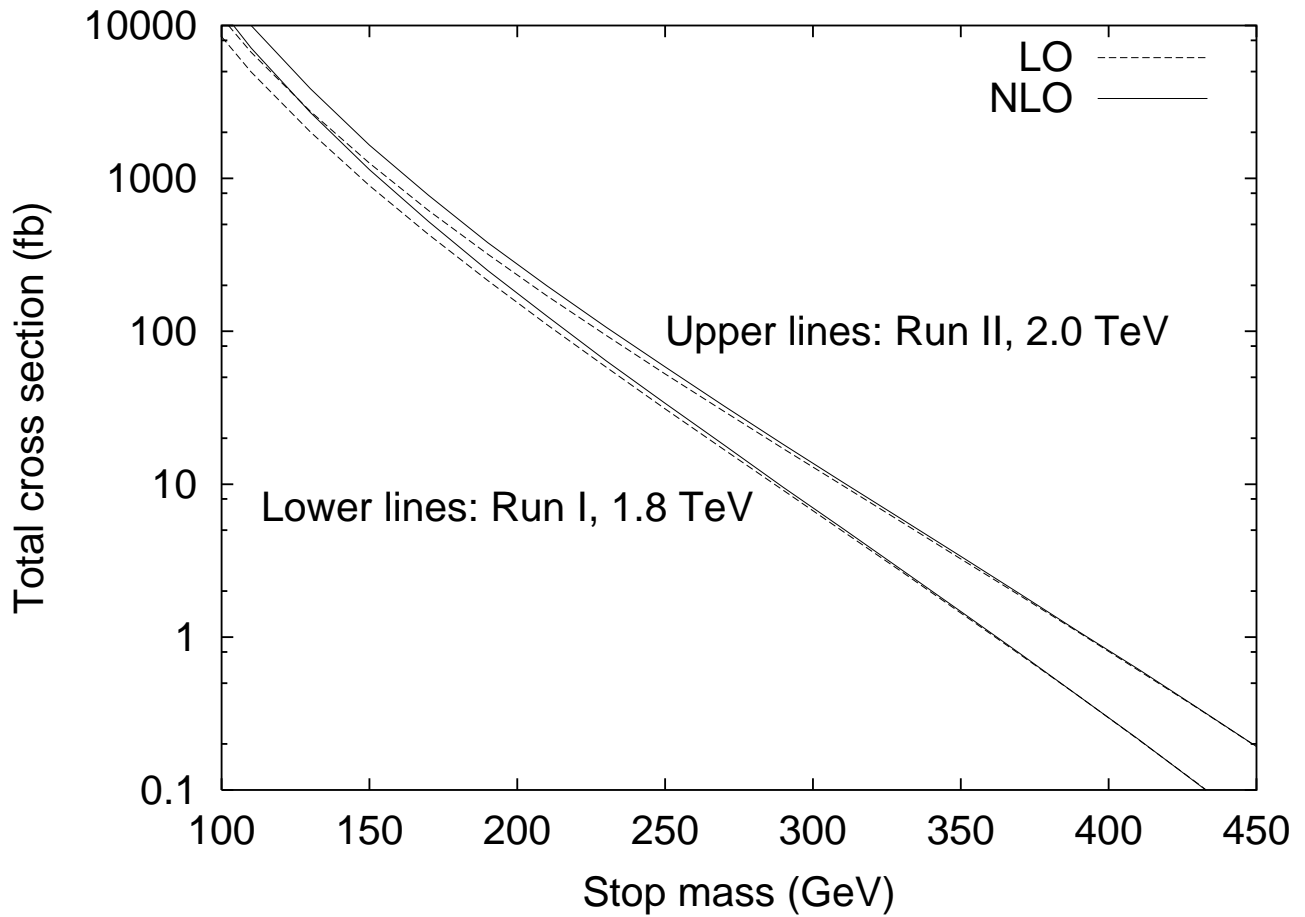


Figure 1: LO and NLO cross sections for stop pair production in $p\bar{p}$ collisions at Tevatron Run I (1.8 TeV) and Run II (2.0 TeV), from PROSPINO [17, 18]. Cross sections are evaluated at the scale $\mu = m_{\tilde{t}}$.

supergravity; in this case SUSY is broken at the Planck scale so that the gravitino plays no role in the collider phenomenology. Then the lightest neutralino is the LSP and ends all superparticle decay chains. The reach of the Tevatron for a number of stop decay modes has been analyzed in Ref. [20]. The signal depends on the decay chain, which in turn depends on the relative masses of various SUSY particles. For sufficiently heavy stops, the decay $\tilde{t} \rightarrow t\tilde{\chi}_1^0$ will dominate. This channel is of limited use at Run II because the stop pair production cross section falls rapidly with increasing stop mass, and this channel requires $m_{\tilde{t}} > m_t + m_{\tilde{\chi}_1^0}$, which is quite heavy for the Tevatron in the case of minimal supergravity.² For lighter stops, if a chargino is lighter than the stop then $\tilde{t} \rightarrow b\tilde{\chi}_1^+$ tends to dominate (followed by the decay of the chargino). The details of the signal depend on the Higgsino content of $\tilde{\chi}_1^+$. If $\tilde{\chi}_1^+$ has a mass larger than $m_{\tilde{t}} - m_b$, the previous decay does not occur and the three-body decay $\tilde{t} \rightarrow bW^+\tilde{\chi}_1^0$ dominates; this decay proceeds through the exchange of a virtual top quark, chargino, or bottom squark. If the stop is too light to decay into an on-shell W boson and $\tilde{\chi}_1^0$, then the flavor-changing decay $\tilde{t} \rightarrow c\tilde{\chi}_1^0$ tends to dominate. Finally, if a sneutrino or slepton is light, then $\tilde{t} \rightarrow b\ell^+\tilde{\nu}_\ell$ or $\tilde{t} \rightarrow b\tilde{\ell}^+\nu_\ell$, respectively, will occur (followed by the decays of the slepton or the sneutrino, if it is not the LSP). At Run II with 2 (20) fb^{-1} of total integrated luminosity, in the context of minimal supergravity one can probe stop masses up to 160 (200) GeV in the case of the flavor changing decay, while stop masses as high as 185 (260) GeV can be probed if the stop decays into a bottom quark and a chargino [20]. A similar reach holds in the case of a light sneutrino [20].

One can also search for stops in the decay products of other SUSY particles [20]. In top decays, the process $t \rightarrow \tilde{t}\tilde{g}$ is already excluded because of the existing lower bound on the gluino mass³. Other possibilities are $\tilde{\chi}^- \rightarrow b\tilde{t}^*$ and $\tilde{g} \rightarrow t\tilde{t}^*$. Finally, the decays $\tilde{b} \rightarrow \tilde{t}W^-$ and $\tilde{t}H^-$ have to compete with the preferred decay, $\tilde{b} \rightarrow b\tilde{\chi}_1^0$, and so may have small branching ratios (depending on the masses of \tilde{t} , \tilde{b} , $\tilde{\chi}_1^0$ and H^-). The signals for these processes at the Tevatron Run II have been considered in minimal supergravity in Ref. [20].

Relatively few studies have been done in the context of low-energy SUSY breaking with a gravitino LSP. A study of GMSB signals performed as part of the Tevatron Run II workshop [7] considered the decays of various SUSY particles as the NLSP. As discussed before, the NLSP in such models will decay directly to the gravitino and Standard Model particles. If the stop is the NLSP in such a model, then it will decay via $\tilde{t} \rightarrow t^{(*)}\tilde{G} \rightarrow bW^+\tilde{G}$ (for $m_{\tilde{t}} > m_b + m_W$). Note that because \tilde{G} is typically very light in such models, $m_{\tilde{t}} > m_W + m_b$ is sufficient for this decay to proceed with an on-shell W boson. Ref. [20] found sensitivity at Run II to this decay mode for stop masses up to 180 GeV with 4 fb^{-1} . This stop decay looks very much like a top quark decay; nevertheless, even for stop masses near m_t , such stop decays

²In low-energy SUSY breaking scenarios, however, the mass range $m_{\tilde{t}} > m_t + m_{\tilde{\chi}_1^0}$ is interesting at Tevatron energies because the distinctive signal allows backgrounds to be reduced to a very low level, as we will show.

³The bound on the gluino mass is, however, model dependent. Under certain conditions, an allowed window exists for gluino masses below the gauge boson masses [21,22].

can be separated from top quark decays at the Tevatron using kinematic correlations among the decay products [23].

Finally, Ref. [9] considered general GMSB signals at the Tevatron of the form $\gamma\gamma \cancel{E}_T + X$. The authors of Ref. [9] provide an analysis of the possible bounds on the stop mass coming from the Run I Tevatron data. They analyze the stop decay mode into a charm quark and a neutralino, and also possible three body decays, by scanning over a sample of models. They conclude that stop masses smaller than 140 GeV can be excluded already by the Run I Tevatron data within low energy supersymmetry breaking models independent of the stop decay mode, assuming that $m_{\tilde{\chi}_1^0} > 70$ GeV.

4 Top squark decay branching ratios

The decay properties of the lighter stop depend on the supersymmetric particle spectrum. Of particular relevance are the mass splittings between the stop and the lightest chargino, neutralino and bottom squark. In our analysis, we assume that the charginos and bottom squarks are heavier than the lighter stop, so that the on-shell decays $\tilde{t} \rightarrow \tilde{b}W$ and $\tilde{t} \rightarrow \tilde{\chi}^+ b$ are kinematically forbidden. Then the details of the stop decay depend on the mass splitting between the stop and the lightest neutralino. If $m_{\tilde{t}} < m_W + m_b + m_{\tilde{\chi}_1^0}$, two decay modes are kinematically accessible:

1. the flavor-changing (FC) two-body decay $\tilde{t} \rightarrow c\tilde{\chi}_1^0$. This two-body decay proceeds through a flavor-changing loop involving W^+ , H^+ or $\tilde{\chi}^+$ exchange or through a tree-level diagram with a $\tilde{t} - \tilde{c}$ mixing mass insertion;
2. the four-body decay via a virtual W boson, $\tilde{t} \rightarrow W^{+*} b \tilde{\chi}_1^0 \rightarrow jjb\tilde{\chi}_1^0$ or $\ell\nu b\tilde{\chi}_1^0$ [24].

The branching ratio of the stop decay into charm and neutralino strongly depends on the details of the supersymmetry breaking mechanism. In models with no flavor violation at the messenger scale, the whole effect is induced by loop effects and receives a logarithmic enhancement which becomes more relevant for larger values of the messenger mass. In the minimal supergravity case, the two-body FC decay branching ratio tends to be the dominant one. In the case of low energy supersymmetry breaking, this is not necessarily the case. Since the analysis of the four-body decay process is very similar to the three-body decay described below for larger mass splittings between the stop and the lighter neutralino, here we shall analyze only the case in which the two-body FC decay $\tilde{t} \rightarrow c\tilde{\chi}_1^0$ is the dominant one whenever $m_{\tilde{t}} < m_W + m_b + m_{\tilde{\chi}_1^0}$.

For larger mass splittings, so that $m_W + m_b + m_{\tilde{\chi}_1^0} < m_{\tilde{t}} < m_t + m_{\tilde{\chi}_1^0}$, the three-body decay $\tilde{t} \rightarrow W^+ b \tilde{\chi}_1^0$ becomes accessible, with $\tilde{\chi}_1^0 \rightarrow \gamma\tilde{G}$. This stop decay proceeds through a virtual top quark, virtual charginos, or virtual sbottoms. Quite generally, this 3-body decay will dominate over the 2-body FC decay in this region of phase space.

For still heavier stops, $m_{\tilde{t}} > m_t + m_{\tilde{\chi}_1^0}$, the two-body tree-level decay mode $\tilde{t} \rightarrow t\tilde{\chi}_1^0$ becomes kinematically accessible and will dominate. Although the 3-body and 2-body FC decays are still present, their branching ratios are strongly suppressed.

Let us emphasize that, since the bino is an admixture of the zino and the photino, a pure bino neutralino can decay into either $\gamma\tilde{G}$ or $Z\tilde{G}$ (see Eq. 1.3). If the lightest neutralino is a mixture of bino and wino components, then the relative zino and photino components can be varied arbitrarily, leading to a change in the relative branching ratios to $\gamma\tilde{G}$ and $Z\tilde{G}$. If the lightest neutralino contains a Higgsino component, then the decay to $h^0\tilde{G}$ is also allowed. We show in Fig. 2 the branching ratio of the lightest neutralino into $\gamma\tilde{G}$ as a function of its mass and Higgsino content.

5 Top squark signals in low-energy SUSY breaking

As discussed in the previous section, the decay properties of the lighter stop depend primarily on the mass splitting between the stop and the lightest neutralino. In this section, we proceed with the phenomenological analysis of the signatures of top squark production associated with the different decay modes. In Sec. 5.1 we shall analyze the signatures associated with the two-body FC decay, which after the neutralino decay leads to $\tilde{t} \rightarrow c\gamma\tilde{G}$. In Sec. 5.2 we shall analyze the signatures associated with the three-body decay, which after neutralino decay leads to $\tilde{t} \rightarrow bW^+\gamma\tilde{G}$. The two-body decay $\tilde{t} \rightarrow t\tilde{\chi}_1^0$, which typically dominates for $m_{\tilde{t}} > m_t + m_{\tilde{\chi}_1^0}$, leads to the same final state as the three-body decay and therefore the discussion of this case will be included in Sec. 5.2. Finally, in Sec. 5.3 we consider the possibility that stops are produced in the decays of top quarks.

5.1 Two-body FC decay: $\tilde{t} \rightarrow c\gamma\tilde{G}$

With the stop undergoing the aforementioned decay, the final state consists of a pair each of charm jets, photons and (invisible) gravitinos. As we will show below, the backgrounds to this process are small enough that we need not require charm tagging. Thus the signal consists of

$$2(\text{jets}) + 2\gamma + \cancel{E}_T.$$

The selection criteria we adopt are:

1. each event must contain two jets and two photons, each of which should have a minimum transverse momentum ($p_T > 20$ GeV) and be contained in the pseudorapidity range $-2.5 < \eta < 2.5$;
2. the jets and the photons should be well separated from each other; namely,

$$\delta R_{jj} > 0.7, \quad \delta R_{\gamma\gamma} > 0.3, \quad \delta R_{j\gamma} > 0.5$$

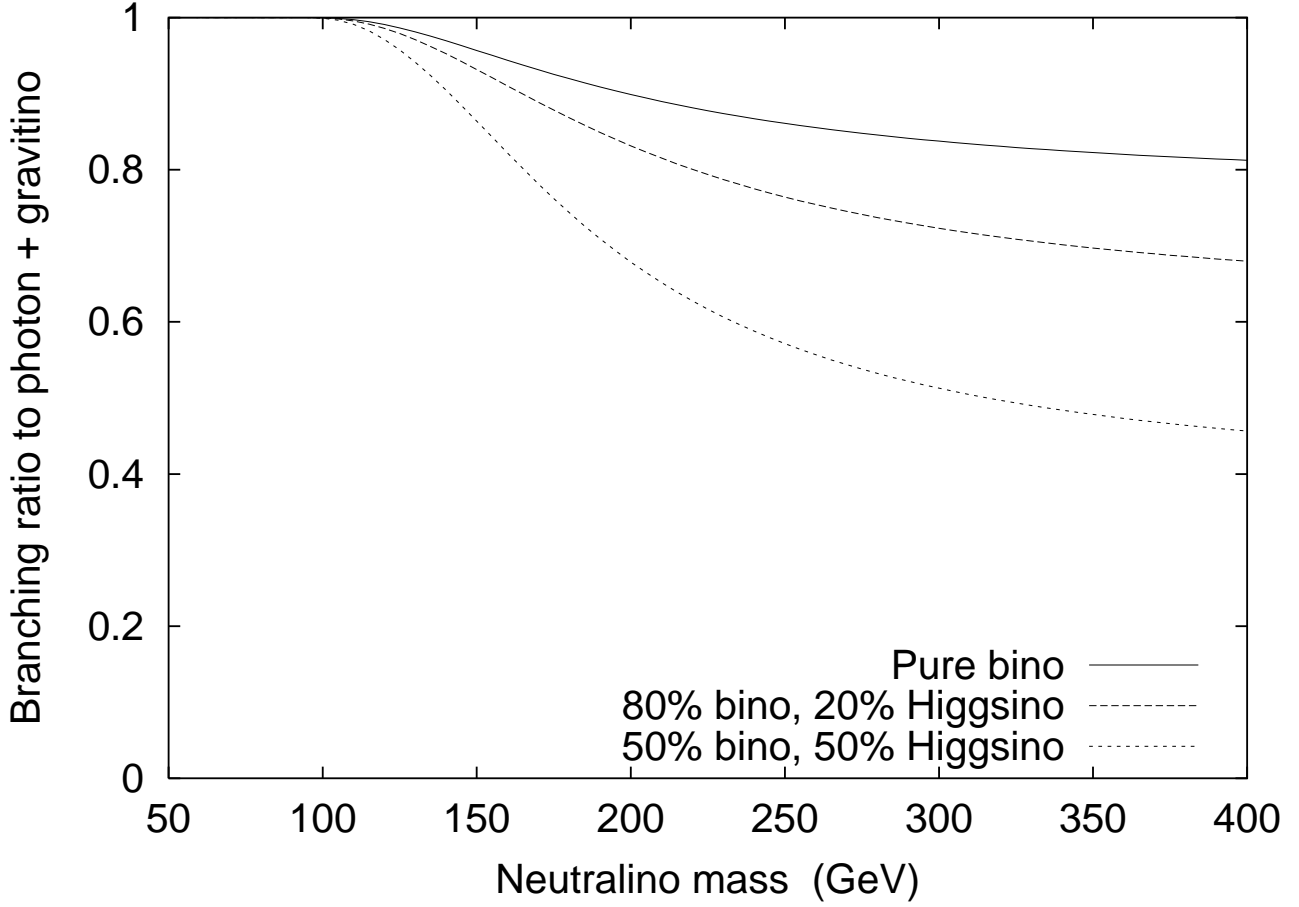


Figure 2: Branching ratio for the decay of the lightest neutralino into a photon and a gravitino as a function of the neutralino mass. Shown are the branching ratio if the neutralino is a pure bino (solid line) and for 20% and 50% Higgsino admixtures (long and short dashed lines, respectively) assuming that $m_{h^0} = 120$ GeV and that the other MSSM Higgs bosons are very heavy. For the Higgsino admixture in the lightest neutralino, we choose the $\tilde{H}_1-\tilde{H}_2$ mixing so that the field content is aligned with that of h^0 and the longitudinal component of the Z boson in order to minimize the branching ratio to photons.

Background	Cross section after cuts	after γ ID
$jj\gamma\gamma Z, Z \rightarrow \nu\bar{\nu}$	~ 0.2 fb	~ 0.13 fb
$jj\gamma\nu\bar{\nu} + \gamma$ radiation	~ 0.002 fb	~ 0.001 fb
$b\bar{b}\gamma\gamma, c\bar{c}\gamma\gamma$	$\lesssim 0.1$ fb	~ 0.06 fb
$jj\gamma\gamma$	~ 0.2 fb	~ 0.13 fb
Backgrounds with fake photons:		
$jj(ee \rightarrow \gamma\gamma)$	$\sim 5 \times 10^{-4}$ fb	$\sim 5 \times 10^{-4}$ fb
$jj\gamma(j \rightarrow \gamma)$	~ 0.8 fb	~ 0.8 fb
$jj(jj \rightarrow \gamma\gamma)$	~ 0.8 fb	~ 0.8 fb
Total	~ 2 fb	~ 2 fb

Table 1: Backgrounds to $t\bar{t}^* \rightarrow jj\gamma\gamma \cancel{E}_T$. The photon identification efficiency is taken to be $\epsilon_\gamma = 0.8$ for each real photon. See text for details.

where $\delta R^2 = \delta\eta^2 + \delta\phi^2$, with $\delta\eta$ ($\delta\phi$) denoting the difference in pseudorapidity (azimuthal angle) of the two entities under consideration;

- the invariant mass of the two jets should be sufficiently far away from the W - and Z -masses:

$$m_{jj} \notin (75 \text{ GeV}, 95 \text{ GeV});$$

- each event should be associated with a minimum missing transverse momentum ($\cancel{p}_T > 30 \text{ GeV}$).

The photons and jets in signal events tend to be very central; in particular, reducing the pseudorapidity cut for the two photons to $-2.0 < \eta < 2.0$ would reduce the signal by less than about 3%. (This change would reduce the background by a somewhat larger fraction.) Apart from ensuring observability, these selection criteria also serve to eliminate most of the backgrounds, which are listed in Table 1.

A primary source of background is the SM production of $jj\gamma\gamma\nu_i\bar{\nu}_i$ where the jets could have arisen from either quarks or gluons in the final state of partonic subprocesses. A full diagrammatic calculation would be very computer-intensive and is beyond the scope of this work. Instead, we consider the subprocesses that are expected to contribute the bulk of this particular background, namely $p\bar{p} \rightarrow 2j + 2\gamma + Z + X$ with the Z subsequently decaying into neutrinos. These processes are quite tractable and were calculated with the aid of the helicity amplitude program MADGRAPH [25]. On imposition of the abovementioned set of cuts, this background at the Run II falls to below ~ 0.2 fb.

An independent estimate of the $jj\gamma\gamma\nu_i\bar{\nu}_i$ background may be obtained through the consideration of the single-photon variant, namely $jj\gamma\nu_i\bar{\nu}_i$ production, a process that MADGRAPH can handle. After imposing the same kinematic cuts (other than requiring only one photon) as above, this process leads to a cross

section of roughly 0.2 fb. Since the emission of a second hard photon should cost us a further power of α_{em} , the electromagnetic coupling constant, this background falls to innocuous levels. We include both this estimate and the one based on Z production from the previous paragraph in Table 1. While a naive addition of both runs the danger of overcounting, this is hardly of any importance given the overwhelming dominance of one.

A second source of background is $b\bar{b}\gamma\gamma$ ($c\bar{c}\gamma\gamma$), with missing transverse energy coming from the semileptonic decay of one or both of the b (c) mesons. In this case, though, the neutrinos tend to be soft due to the smallness of the b and c masses. Consequently, the cut on \cancel{p}_T serves to eliminate most of this background, leaving behind less than 0.1 fb. This could be further reduced (to $\lesssim 0.001$ fb) by vetoing events with leptons in association with jets. However, such a lepton veto would significantly impact the selection efficiency of our signal, which contains $c\bar{c}$, thereby reducing our overall sensitivity in this channel.

A third source of background is $jj\gamma\gamma$ production, in which the jet (light quark or gluon) and/or photon energies are mismeasured leading to a fake \cancel{p}_T . To simulate the effect of experimental resolution, we use a (very pessimistic) Gaussian smearing: $\delta E_j/E_j = 0.1 + 0.6/\sqrt{E_j(\text{GeV})}$ for the jets and $\delta E_\gamma/E_\gamma = 0.05 + 0.3/\sqrt{E_\gamma(\text{GeV})}$ for the photons.⁴ While the production cross section is much higher than that of any of the other backgrounds considered, the ensuing missing momentum tends to be small; in particular, our cut on \cancel{E}_T reduces this background by almost 99%.⁵ On imposition of our cuts, this fake background is reduced to ~ 0.2 fb.⁶

Finally, we consider the instrumental backgrounds from electrons or jets misidentified as photons. Based on Run I analyses [27] of electron pair production and taking the probability for an electron to fake a photon to be about 0.4%, we estimate the background due to electrons faking photons to be of order 5×10^{-4} fb. More important is the background in which a jet fakes a photon. Based on a Run I analysis [26] and taking the probability for a jet to fake a photon to be about 0.1%, we estimate the background due to $jjj\gamma$ in which one of the jets fakes a second photon to be about 0.8 fb. Similarly, we estimate that the background due to $jjjj$ in which two of the jets fake photons is somewhat smaller; to be conservative we take it to be of the same order, *i.e.*, 0.8 fb.

Having established that the backgrounds are small, let us now turn to the signal cross section that survives the cuts. In Fig. 3, we present these as contours in the $m_{\tilde{t}}-m_{\tilde{\chi}_1^0}$ plane. We assume that the branching ratio of $\tilde{t} \rightarrow c\tilde{\chi}_1^0$ dominates in the region of parameter space that we consider here. The

⁴We have also performed similar smearing for the other background channels as well as for the signal. However, there it hardly is of any importance as far as the estimation of the total cross section is concerned.

⁵This reduction factor is in rough agreement with that found for $\gamma + j$ events in CDF Run I data in Ref. [26].

⁶We note that in the squark searches in supergravity scenarios the signal is $jj \cancel{E}_T$; in this case a similar background due to dijet production with fake \cancel{p}_T is present. This background is larger by two powers of α than the $jj\gamma\gamma$ background, yet it can still be reduced to an acceptable level by a relatively hard cut on \cancel{p}_T (see, *e.g.*, Ref. [20]).

branching ratio of $\tilde{\chi}_1^0 \rightarrow \gamma\tilde{G}$ is taken from Fig. 2 assuming that $\tilde{\chi}_1^0$ is a pure bino.⁷ All our plots are made before detector efficiencies are applied. With a real detector, each photon is identified with about $\epsilon_\gamma = 80\%$ efficiency; thus the cross sections shown in Fig. 3 must be multiplied by $\epsilon_\gamma^2 = 0.64$ in order to obtain numbers of events.⁸ While the production cross sections are independent of the neutralino mass, the decay kinematics have a strong dependence on $m_{\tilde{\chi}_1^0}$. For a given $m_{\tilde{t}}$, a small mass splitting between $m_{\tilde{t}}$ and $m_{\tilde{\chi}_1^0}$ would imply a soft charm jet, which would often fail to satisfy our selection criteria. This causes the gap between the cross section contours and the upper edge of the parameter space band that we are exploring in Fig. 3. This is further compounded at large $m_{\tilde{\chi}_1^0}$ by the fact that a large neutralino mass typically implies a smaller $\tilde{\chi}_1^0 \rightarrow \gamma\tilde{G}$ branching fraction (see Fig.2). On the other hand, a small $m_{\tilde{\chi}_1^0}$ results in reduced momenta for the gravitino and the photon, once again resulting in a loss of signal; however, this is important only for $m_{\tilde{\chi}_1^0} \lesssim 70$ GeV, which is not relevant in this search channel.

The signal cross sections are fairly substantial. In particular, the dark area in Fig. 3 corresponds to a signal cross section of 50 fb or larger at Run I of the Tevatron. Taking into account the identification efficiency of 64% for the two photons, such a cross section would have yielded 3 signal events in the 100 pb⁻¹ collected in Run I over a background of much less than 1 event. Run I can thus exclude this region at 95% confidence level. In particular, we conclude that Run I data excludes stop masses up to about 200 GeV, for large enough mass splitting between the stop and the neutralino. When the stop-neutralino mass splitting is small (*i.e.*, less than about 10 – 20 GeV), the charm quark jets become too soft and the signal efficiency decreases dramatically. For comparison, a $D\bar{O}$ search [28] for inclusive $p\bar{p} \rightarrow \tilde{\chi}_2^0 + X$ with $\tilde{\chi}_2^0 \rightarrow \gamma\tilde{\chi}_1^0$ in the context of minimal supergravity yields a limit on the production cross section of about 1 pb for parent squark masses of order 150-200 GeV. Interpreting this in terms of stop pair production with $\tilde{\chi}_2^0 \rightarrow \gamma\tilde{\chi}_1^0$ reidentified as $\tilde{\chi}_1^0 \rightarrow \gamma\tilde{G}$ increases the signal efficiency by a factor of ~ 2.7 because every SUSY event now contains two photons [28]; the $D\bar{O}$ analysis then yields a stop mass bound of about 180 GeV, in rough agreement with our result.⁹ In addition, Ref. [9] projected a Run I exclusion of stops in this decay channel for masses below about 160-170 GeV, again in rough agreement with our result.

To claim a discovery at the 5σ level, one must observe a large enough number of events that the probability for the background to fluctuate up to that level is less than 5.7×10^{-7} . Because the number of expected background events in this analysis is small, we use Poisson statistics to find the number of signal events required for a 5σ discovery. Taking the total background cross section to be 2 fb from Table 1, we show in Table 2 the expected maximum stop discovery mass reach at Tevatron Run II for various amounts

⁷If $\tilde{\chi}_1^0$ is not a pure bino, its branching ratio to $\gamma\tilde{G}$ will typically be reduced somewhat when its mass is large (see Fig. 2). This will lead to a reduction of the signal cross section at large $m_{\tilde{\chi}_1^0}$ by typically a few tens of percent.

⁸The diphoton trigger efficiency is close to 100%, so we neglect it here.

⁹Note, however, that the non-negligible mass of the LSP of about 35 GeV assumed in Ref. [28] leads to kinematics that differ significantly from those in our analysis, in which the gravitino is essentially massless.

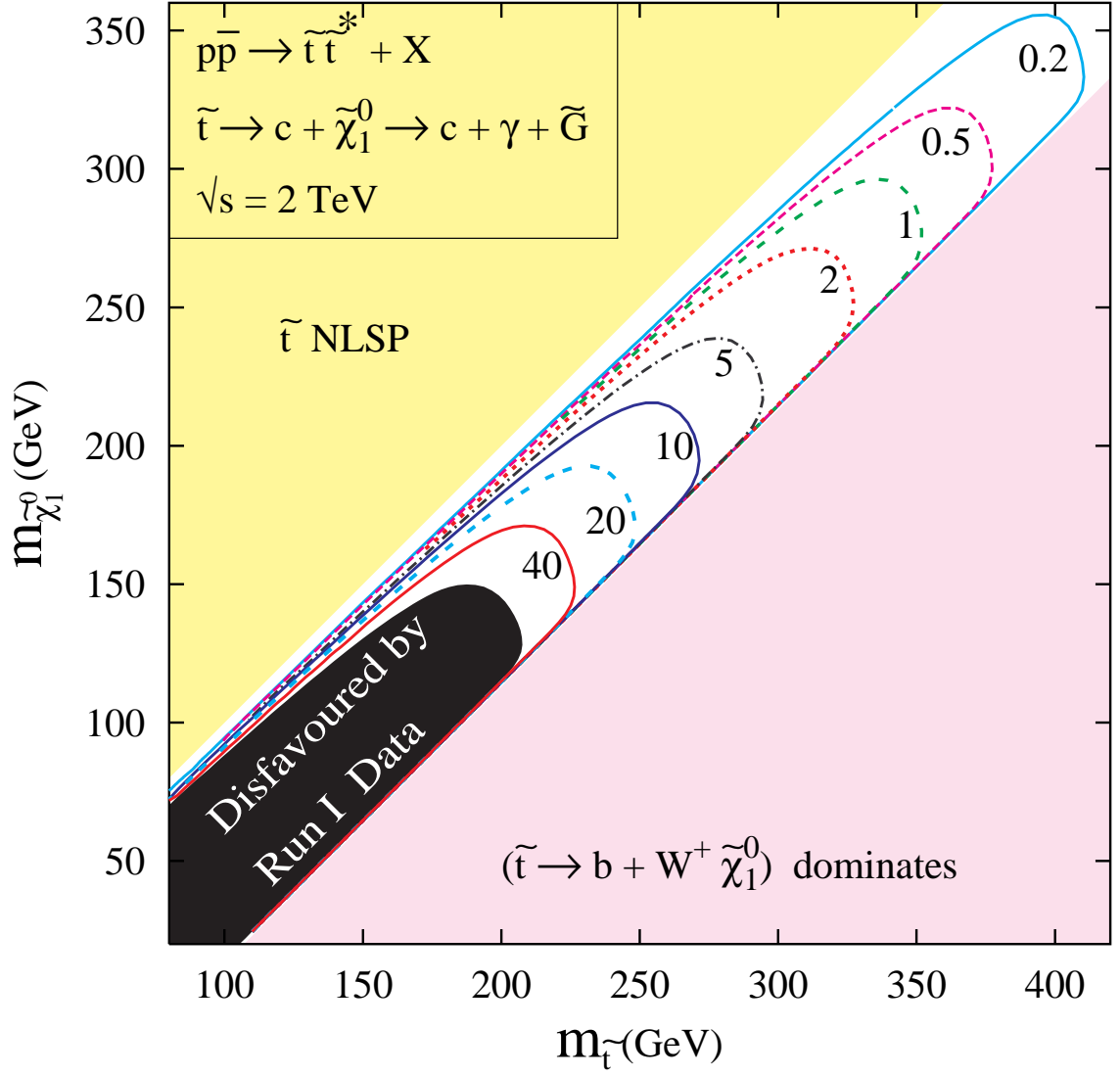


Figure 3: Cross sections in fb for stop pair production in Run II with $\tilde{t} \rightarrow c\gamma\tilde{G}$, after cuts. No efficiencies have yet been applied. The black area is excluded by non-observation of $jj\gamma\gamma\not{E}_T$ events in Run I.

$\int \mathcal{L}$	B	S for a 5σ discovery	$\sigma_S \times \epsilon_\gamma^2$	Maximum stop mass reach
2 fb^{-1}	4	14	7.0 fb	265 GeV
4 fb^{-1}	8	18	4.5 fb	285 GeV
15 fb^{-1}	30	31	2.1 fb	310 GeV
30 fb^{-1}	60	42	1.4 fb	325 GeV

Table 2: Number of signal events (S) required for a 5σ stop discovery at Tevatron Run II in the $jj\gamma\gamma\not{E}_T$ channel and the corresponding signal cross section after cuts and efficiencies and maximum stop mass reach. We assume a photon identification efficiency of $\epsilon_\gamma = 0.80$. The number of background events (B) is based on a background cross section of 2 fb from Table 1.

of integrated luminosity.¹⁰ In particular, with 4 fb^{-1} a stop discovery can be expected in this channel if $m_{\tilde{t}} < 285 \text{ GeV}$, with S/B of more than $2/1$.¹¹ Including the effects of mixing in the composition of the lightest neutralino, a 50% reduction in the $\tilde{\chi}_1^0 \rightarrow \gamma\tilde{G}$ branching ratio compared to the pure bino case would reduce the stop mass reach by only about 20 GeV. For such a reduction to occur in the relevant neutralino mass range of about 200 – 250 GeV, the lightest neutralino would have to be less than half bino.

5.2 Three-body decay: $\tilde{t} \rightarrow bW^+\gamma\tilde{G}$

For a large enough splitting between the stop and neutralino masses, the signature of stop pair production would be¹² $jjWW\gamma\gamma\not{E}_T$. In this analysis, we consider only the dominant hadronic decay mode of both W bosons.

This decay mode of the stop proceeds via three Feynman diagrams, involving an intermediate off-shell top quark, chargino or sbottom. We use the full decay matrix elements as given in Ref. [29]. Although this introduces several additional parameters into the analysis, a few simplifying assumptions may be made without becoming too model dependent. For example, assuming that the lightest stop is predominantly the superpartner of the right-handed top-quark (\tilde{t}_R), eliminates the sbottom exchange diagram altogether. Even if the stop contains a mixture of \tilde{t}_R and \tilde{t}_L , under our assumption that the lighter stop is the next-to-lightest Standard Model superpartner, the sbottom exchange diagram will be suppressed by the necessarily

¹⁰The cross sections and numbers of events required for discovery are quoted in terms of integrated luminosities at a single detector. If data from the CDF and DØ detectors are combined, the integrated luminosity of the machine is effectively doubled.

¹¹For comparison, in the case of minimal supergravity a reach of $m_{\tilde{t}} < 180 \text{ GeV}$ can be expected in the $\tilde{t} \rightarrow c\tilde{\chi}_1^0$ channel with 4 fb^{-1} at Tevatron Run II; the same reach is obtained in low-energy SUSY breaking scenarios in which the stop is the NLSP rather than the neutralino [20]. In both of these cases, the signal consists of $jj\not{E}_T$, with no photons in the final state.

¹²The backgrounds are again small enough after cuts in this channel that we do not need to tag the b quarks. In the case of a discovery, one could imagine tagging the b quarks and reconstructing the W bosons in order to help identify the discovered particle.

larger sbottom mass. As for the chargino exchange, the wino component does not contribute for a \tilde{t}_R decay. Thus the chargino contribution is dominated by its Higgsino component. Furthermore, if we concentrate on scenarios with large values of the supersymmetric mass parameter μ and of the wino mass parameter (in which case the charginos are heavy and the neutralino is almost a pure bino), the chargino exchange contribution is also suppressed and the dominant decay mode is via the diagram involving an off-shell top quark. To simplify our numerical calculations, we have then assumed that only this diagram contributes to the stop decay matrix element. We have checked for a few representative points though, that the inclusion of the sbottom and chargino diagrams does not significantly change the signal efficiency after cuts as long as we require that $m_{\tilde{b}}, m_{\tilde{\chi}^+} > m_{\tilde{t}}$.

As the W bosons themselves decay, it might be argued that their polarization information needs to be retained. However, since we do not consider angular correlations between the decay products, this is not a crucial issue; the loss of such information at intermediate steps in the decay does not lead to a significant change in the signal efficiency after cuts. This is particularly true for the hadronic decay modes of the W , for which the profusion of jets frequently leads to jet overlap, thereby obscuring detailed angular correlations. It is thus safe to make the approximation of neglecting the polarization of the W bosons in their decay distributions, and we do so in our analysis.

Before we discuss the signal profile and the backgrounds, let us elaborate on the aforementioned jet overlapping. With six quarks in the final state, some of the resultant jets will very often be too close to each other to be recognizable as coming from different partons. We simulate this as follows. We count a final-state parton (quark or gluon) as a jet only if it has a minimum energy of 5 GeV and lies within the pseudorapidity range $-3 < \eta < 3$. We then merge any two jets that fall within a δR separation of 0.5; the momentum of the resultant jet is the sum of the two momenta. We repeat this process iteratively, starting with the hardest jet. Our selection cuts are then applied to the (merged) jets that survive this algorithm.

The signal thus consists of:

$$n \text{ jets} + 2\gamma + \cancel{E}_T \quad (n \leq 6)$$

Hence, all of the SM processes discussed in the previous section yield backgrounds to this signal when up to four additional jets are radiated. Now, the radiation of each hard and well separated jet suppresses the cross section by a factor of order $\alpha_s \simeq 0.118$. Then, since the $jj\gamma\gamma \cancel{E}_T$ backgrounds are already quite small after the cuts applied in the previous section (see Table 1), the backgrounds with additional jets are expected to be still smaller.¹³

There exists a potential exception to the last assertion, namely the background due to $t\bar{t}\gamma\gamma$ production. To get an order of magnitude estimate, the cross section for $t\bar{t}$ production at Tevatron Run II is 8 pb [30]. If both of the photons are required to be energetic and isolated, we would expect a suppression by a factor

¹³For the backgrounds in which one or both of the photons are faked by misidentified jets, we have taken into account the larger combinatoric factor that arises when more jets are present to be misidentified.

of order α_{em}^2 , leading to a cross section of the order of 0.5 fb. This cross section is large enough that we need to consider it carefully.

If both W bosons were to decay hadronically, then a sufficiently large missing transverse energy can only come from a mismeasurement of the jet or photon energies. As we have seen in the previous section, this missing energy is normally too small to pass our cuts, thereby suppressing the background. If one of the W bosons decays leptonically, however, it will yield a sizable amount of \cancel{E}_T . This background can be largely eliminated by requiring that no lepton (e or μ) is seen in the detector. This effectively eliminates the W decays into e or μ or decays to τ followed by leptonic τ decays; the remaining background with hadronic τ decays is naturally quite small without requiring additional cuts. Considerations such as these lead us to an appropriate choice of criteria for an event to be selected:

1. At least four jets, each with a minimum transverse momentum $p_{Tj} > 20$ GeV and contained in the pseudorapidity interval of $-3 < \eta_j < 3$. Any two jets must be separated by $\delta R_{jj} > 0.7$. As most of the signal events do end up with 4 or more energetic jets (the hardest jets coming typically from the W boson decays), this does not cost us in terms of the signal, while reducing the QCD background significantly. In addition, the $t\bar{t}\gamma\gamma$ events with both W 's decaying leptonically are reduced to a level of order 10^{-4} fb by this requirement alone.
2. Two photons, each with $p_{T\gamma} > 20$ GeV and pseudorapidity $-2.5 < \eta_\gamma < 2.5$. The two photons must be separated by at least $\delta R_{\gamma\gamma} > 0.3$.
3. Any photon-jet pair must have a minimum separation of $\delta R_{j\gamma} > 0.5$.
4. A minimum missing transverse energy $\cancel{E}_T > 30$ GeV.
5. The event should not contain any isolated lepton with $p_T > 10$ GeV and lying within the pseudorapidity range $-3 < \eta < 3$.

As in the previous section, the cut on \cancel{E}_T serves to eliminate most of the background events with only a fake missing transverse momentum (arising out of mismeasurement of jet energies). In association with the lepton veto, it also eliminates the bulk of events in which one of the W bosons decays leptonically (including the τ channel). A perusal of Table 3, which summarizes the major backgrounds after cuts, convinces us that the backgrounds to this channel are very small, in fact much smaller than those for the previous channel.

The signal cross section after cuts (but before photon identification efficiencies) is shown in Fig. 4 as a function of the stop and $\tilde{\chi}_1^0$ masses. We assume that the branching ratio of $\tilde{t} \rightarrow bW\tilde{\chi}_1^0$ dominates in the region of parameter space under consideration. The branching ratio of $\tilde{\chi}_1^0 \rightarrow \gamma\tilde{G}$ is again taken from Fig. 2 assuming that $\tilde{\chi}_1^0$ is a pure bino. The signal efficiency after cuts is about 45%. For small neutralino masses

Background	Cross section after cuts	after γ ID
$(jj\gamma\gamma Z, Z \rightarrow \nu\bar{\nu}) + 2j$	~ 0.003 fb	~ 0.002 fb
$jj\nu\bar{\nu}\gamma\gamma + 2j$	$\sim 3 \times 10^{-5}$ fb	$\sim 2 \times 10^{-5}$ fb
$(b\bar{b}\gamma\gamma, c\bar{c}\gamma\gamma) + 2j$	~ 0.001 fb	~ 0.0006 fb
$jj\gamma\gamma + 2j$	$\lesssim 0.003$ fb	$\lesssim 0.002$ fb
$t\bar{t}\gamma\gamma, WW \rightarrow jjjj$	$\lesssim 10^{-4}$ fb	$\lesssim 10^{-4}$ fb
$t\bar{t}\gamma\gamma, WW \rightarrow jj\ell\nu, \ell = e, \mu, \text{ or } \tau \rightarrow \ell$	~ 0.001 fb	~ 0.0006 fb
$t\bar{t}\gamma\gamma, WW \rightarrow jj\tau\nu, \tau \rightarrow j$	$\lesssim 0.01$ fb	$\lesssim 0.006$ fb
Backgrounds with fake photons:		
$jj(ee \rightarrow \gamma\gamma) + 2j$	$\sim 7 \times 10^{-6}$ fb	$\sim 7 \times 10^{-6}$ fb
$jj\gamma(j \rightarrow \gamma) + 2j$	~ 0.02 fb	~ 0.02 fb
$jj(jj \rightarrow \gamma\gamma) + 2j$	~ 0.03 fb	~ 0.03 fb
Total	$\lesssim 0.07$ fb	~ 0.06 fb

Table 3: Backgrounds to $\tilde{t}\tilde{t}^* \rightarrow jjWW\gamma\gamma \cancel{E}_T$ with both W bosons decaying hadronically. The photon identification efficiency is taken to be $\epsilon_\gamma = 0.8$ for each real photon. See text for details.

($m_{\tilde{\chi}_1^0} \lesssim 50$ GeV), though, both the photons and the gravitinos (\cancel{E}_T) tend to be soft, leading to a decrease in the signal efficiency. For small stop masses (as well as for large stop masses when the stop-neutralino mass difference is small), on the other hand, the jets are soft leading to a suppression of the signal cross section after cuts. As one would expect, both of these effects are particularly pronounced in the contours corresponding to large values of the cross section. The additional distortion of the contours for large neutralino masses can, once again, be traced to the suppression of the $\tilde{\chi}_1^0 \rightarrow \gamma\tilde{G}$ branching fraction (see Fig. 2).

The non-observation of $jjWW\gamma\gamma \cancel{E}_T$ events at Run I of the Tevatron already excludes the region of parameter space shown in black in Fig. 4. As in the previous section, in this excluded region at least 3 signal events would have been produced after cuts and detector efficiencies in the 100 pb^{-1} of Run I data, with negligible background. In particular, Run I data excludes stop masses below about 200 GeV, for neutralino masses larger than about 50 GeV.

We show in Table 4 the expected maximum stop discovery mass reach at Tevatron Run II for various amounts of integrated luminosity.¹⁴ In particular, with 4 fb^{-1} , a stop discovery can be expected in this channel if $m_{\tilde{t}} < 320$ GeV.¹⁵ If the lightest neutralino is not a pure bino, the reach at large neutralino

¹⁴Again, if data from the CDF and D0 detectors are combined, the integrated luminosity of the machine is effectively doubled.

¹⁵For comparison, in the case of minimal supergravity a reach of $m_{\tilde{t}} < 190$ GeV can be expected in the $\tilde{t} \rightarrow bW\tilde{\chi}_1^0$ channel

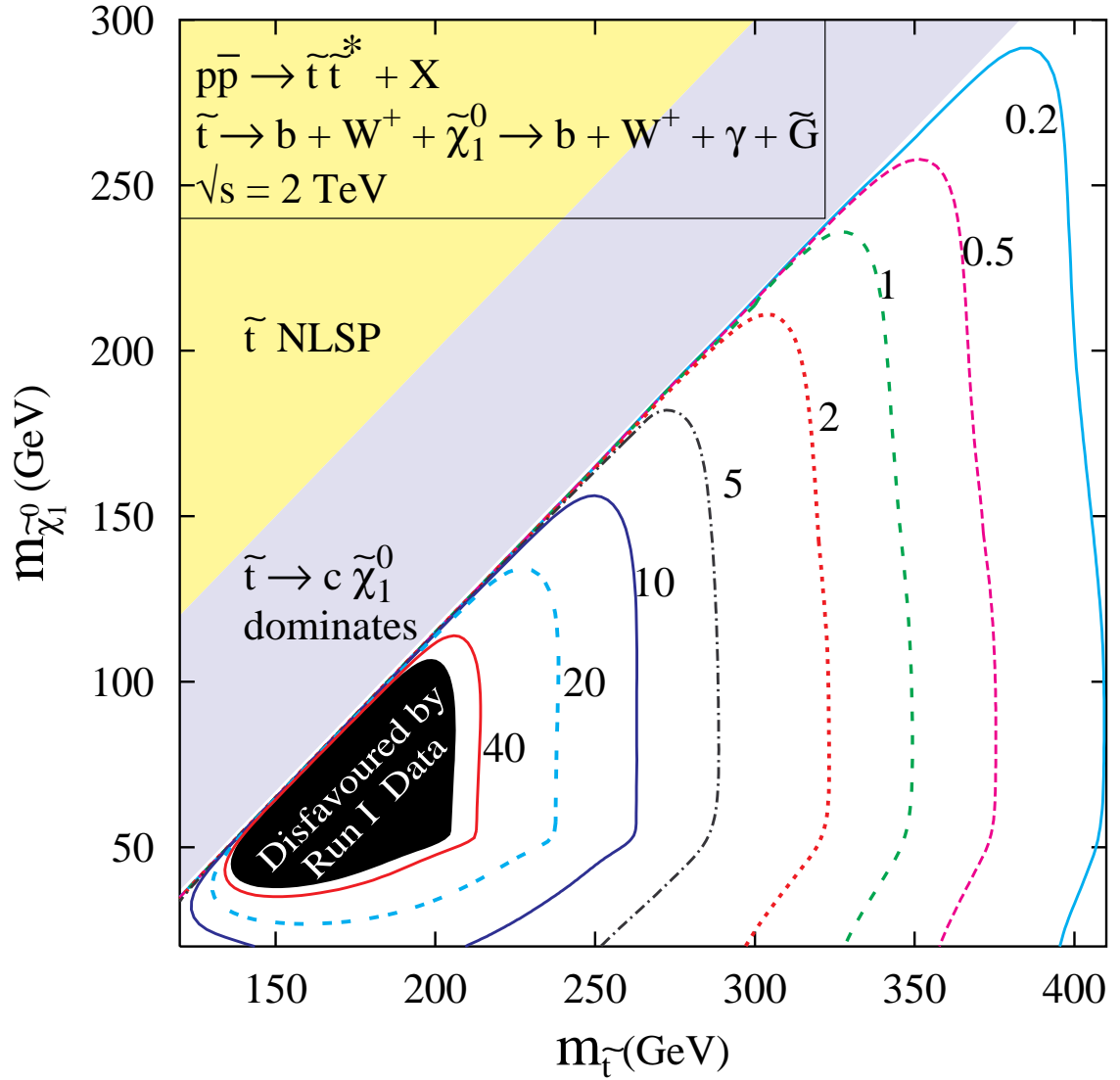


Figure 4: Cross section in fb for stop pair production with $\tilde{t} \rightarrow bW\gamma\tilde{G}$, after cuts. Both W bosons are assumed to decay hadronically. The black area is excluded by non-observation of $jjWW\gamma\gamma\not{E}_T$ events in Run I.

$\int \mathcal{L}$	B	S for a 5σ discovery	$\sigma_S \times \epsilon_\gamma^2$	Maximum stop mass reach
2 fb^{-1}	0.1	5	2.5 fb	300 GeV
4 fb^{-1}	0.2	6	1.5 fb	320 GeV
15 fb^{-1}	0.9	8	0.53 fb	355 GeV
30 fb^{-1}	1.8	10	0.33 fb	375 GeV

Table 4: Number of signal events (S) required for a 5σ stop discovery at Tevatron Run II in the $jjWW\gamma\gamma / E_T$ channel and the corresponding signal cross section after cuts and efficiencies and maximum stop mass reach. We take $\epsilon_\gamma = 0.80$. The number of background events (B) is based on a background cross section of 0.06 fb from Table 3.

masses will be reduced. However, the maximum stop mass reach quoted here will not be affected, because it occurs for $m_{\tilde{\chi}_1^0} \sim 50 - 100$ GeV; in this mass range the lightest neutralino decays virtually 100% of the time to $\gamma\tilde{G}$ due to the kinematic suppression of all other possible decay modes, unless its photino component is fine-tuned to be tiny.

Including a separate analysis of stop production and decay with one or more of the W bosons decaying leptonically would yield an increase in the overall signal statistics; however, we do not expect this increase to dramatically alter the stop discovery reach.

5.3 Stop production in top quark decays

If $m_{\tilde{t}} + m_{\tilde{\chi}_1^0} < m_t$, then stops can be produced in the decays of top quarks. As we will explain here, most of the parameter space in this region is excluded by the non-observation of stop events via direct production or in top quark decays at Run I of the Tevatron. However, some interesting parameter space for this decay remains allowed after Run I, especially if the lighter stop is predominantly \tilde{t}_L .

For $m_{\tilde{t}} < m_b + m_W + m_{\tilde{\chi}_1^0}$, so that the stop decays via $\tilde{t} \rightarrow c\tilde{\chi}_1^0$, the region in which $t \rightarrow \tilde{t}\tilde{\chi}_1^0$ is possible is almost entirely excluded by the limit on stop pair production at Run I, as shown in Fig. 3. A sliver of parameter space in which the stop-neutralino mass splitting is smaller than about 10 GeV remains unexcluded. For $m_{\tilde{t}} > m_b + m_W + m_{\tilde{\chi}_1^0}$, so that the stop decays via $\tilde{t} \rightarrow bW\tilde{\chi}_1^0$, the signal efficiency in the search for direct stop production is degraded for light neutralinos with masses below about 50 GeV and for stops lighter than about 150 GeV. This prevents Run I from being sensitive to stop pair production in the region of parameter space in which top quark decays to stops are possible with the stops decaying to $bW\tilde{\chi}_1^0$, as shown in Fig. 4. In what follows, we focus on this latter region of parameter space.

As discussed before, if the lightest neutralino is mostly bino, the constraints on its mass are model-dependent. The constraints from Tevatron Run I are based on inclusive chargino and neutralino produc-

with 4 fb^{-1} at Tevatron Run II [20].

tion [9,31] under the assumption of gaugino mass unification; the cross section is dominated by production of $\tilde{\chi}_1^\pm \tilde{\chi}_1^\mp$ and $\tilde{\chi}_1^\pm \tilde{\chi}_2^0$. If the assumption of gaugino mass unification is relaxed, then Run I puts no constraint on the mass of $\tilde{\chi}_1^0$. At LEP, while the pair production of a pure bino leads to an easily detectable diphoton signal, it proceeds only via t -channel selectron exchange. The mass bound on a bino $\tilde{\chi}_1^0$ from LEP thus depends on the selectron mass [13]. In particular, for selectrons heavier than about 600 GeV, bino masses down to 20 GeV are still allowed by the LEP data. If $\tilde{\chi}_1^0$ contains a Higgsino admixture, it couples to the Z and can be pair-produced at LEP via Z exchange. For an NLSP with mass between 20 and 45 GeV, as will be relevant in our top quark decay analysis, the LEP search results limit the \tilde{H}_2 component to be less than 1%. Such a small \tilde{H}_2 admixture has no appreciable effect on the top quark partial width to $\tilde{t}\tilde{\chi}_1^0$. We thus compute the partial width for $t \rightarrow \tilde{t}\tilde{\chi}_1^0$ assuming that the neutralino is a pure bino. Taking the lighter stop to be $\tilde{t}_1 = \tilde{t}_L \cos \theta_{\tilde{t}} + \tilde{t}_R \sin \theta_{\tilde{t}}$, we find,

$$\Gamma(t \rightarrow \tilde{t}_1 \tilde{B}) = \left[\frac{4}{9} \sin^2 \theta_{\tilde{t}} + \frac{1}{36} \cos^2 \theta_{\tilde{t}} \right] \frac{\alpha}{\cos^2 \theta_W} \frac{E_{\tilde{B}}}{m_t} \sqrt{E_{\tilde{B}}^2 - m_{\tilde{B}}^2}, \quad (5.1)$$

where $E_{\tilde{B}} = (m_{\tilde{t}}^2 + m_{\tilde{B}}^2 - m_{\tilde{t}}^2)/2m_t$. The numerical factors in the square brackets in Eq. 5.1 come from the hypercharge quantum numbers of the two stop electroweak eigenstates. Clearly, the partial width is maximized if the lighter stop is a pure \tilde{t}_R state; it drops by a factor of 16 if the lighter stop is a pure \tilde{t}_L state. In any case, the branching ratio for $t \rightarrow \tilde{t}\tilde{B}$ does not exceed 6% for $m_{\tilde{t}} > 100$ GeV and $m_{\tilde{\chi}_1^0} > 20$ GeV.¹⁶

The signal from top quark pair production followed by one top quark decaying as in the Standard Model and the other decaying to $\tilde{t}\tilde{\chi}_1^0$, followed by the stop 3-body decay and the neutralino decays to $\gamma\tilde{G}$, is $bbWW\gamma\gamma\not{E}_T$. This signal is the same (up to kinematics) as that from stop pair production in the 3-body decay region. As in the case of stop pair production followed by the 3-body decay, we expect that the background to this process can be reduced to a negligible level. Run I can then place 95% confidence level exclusion limits on the regions of parameter space in which 3 or more signal events are expected after cuts and efficiencies are taken into account. Using the Run I top quark pair production cross section of 6 pb [30] and a total luminosity of 100 pb⁻¹, we compute the number of signal events as a function of the stop and neutralino masses and the stop composition, assuming various values of the signal efficiency after cuts and detector efficiencies. If $\tilde{t}_1 = \tilde{t}_R$, then Run I excludes most of the parameter space below the kinematic limit for this decay even for fairly low signal efficiency $\sim 20\%$, as shown in Fig. 5. If $\tilde{t}_1 = \tilde{t}_L$, on the other hand, the signal cross section is much smaller and Run I gives no exclusion unless the signal efficiency is larger than 75%, which would already be unfeasible including only the identification efficiencies for the two photons; even 100% signal efficiency would only yield an exclusion up to $m_{\tilde{t}} \simeq 118$ GeV.

At Run II, the top quark pair production cross section is 8 pb [30] and the expected total luminosity

¹⁶For neutralino masses below m_Z , as are relevant here, the branching ratio into $\gamma\tilde{G}$ is virtually 100% (see Fig. 2), almost independent of the neutralino composition.

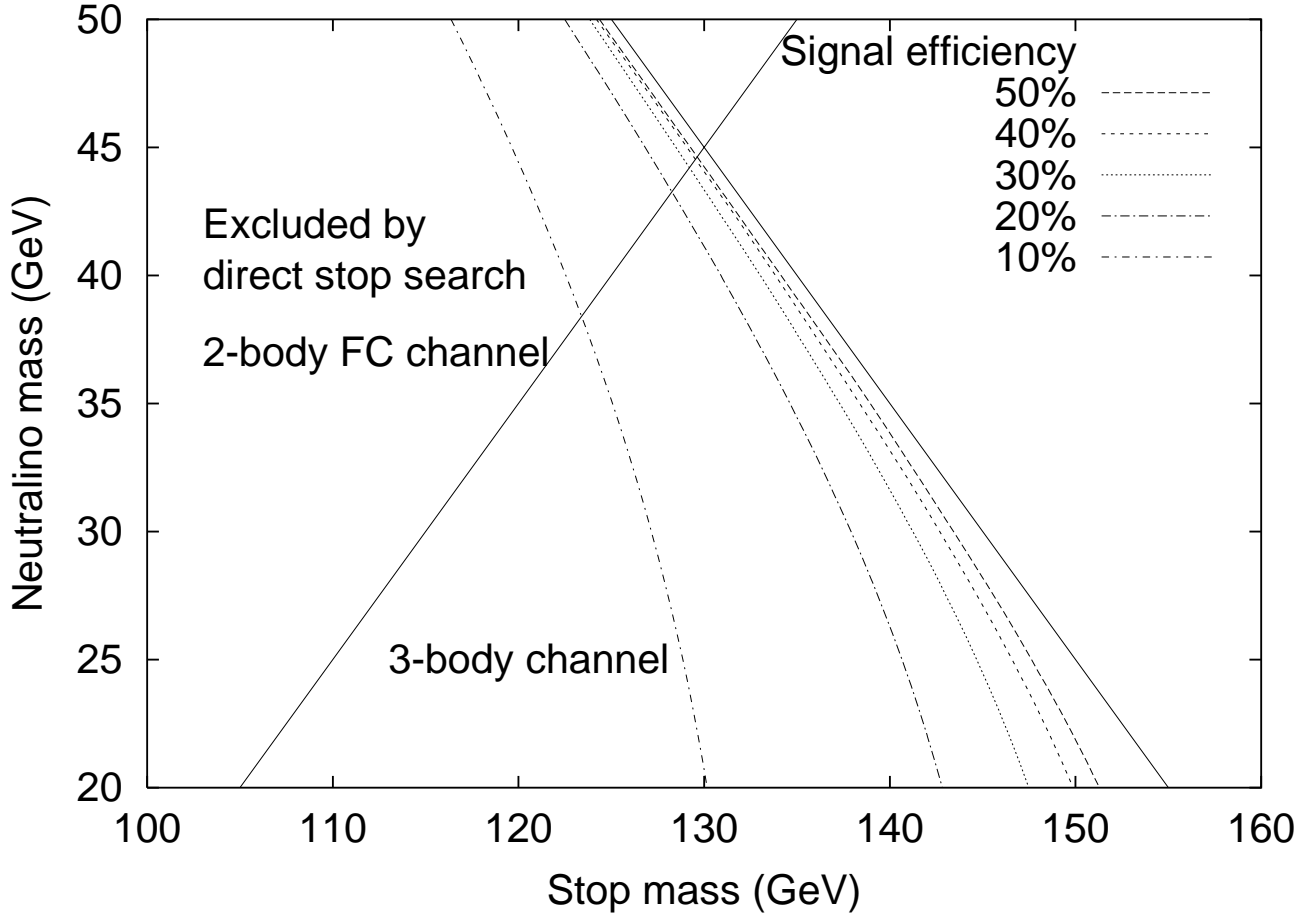


Figure 5: 95% confidence level exclusion limits for top quark decays to stops from Run I for various signal efficiencies, in the case that $\tilde{t}_1 = \tilde{t}_R$, which gives the largest event rates. The area to the left of the curves is excluded. The case $\tilde{t}_1 = \tilde{t}_L$ gives no exclusion for the signal efficiencies considered and is not shown here. The solid line from upper left to lower right is the kinematic limit for $m_t = 175$ GeV. The solid line from upper right to lower left separates the regions in which the 2-body FC decay and the 3-body decay of the stop dominate.

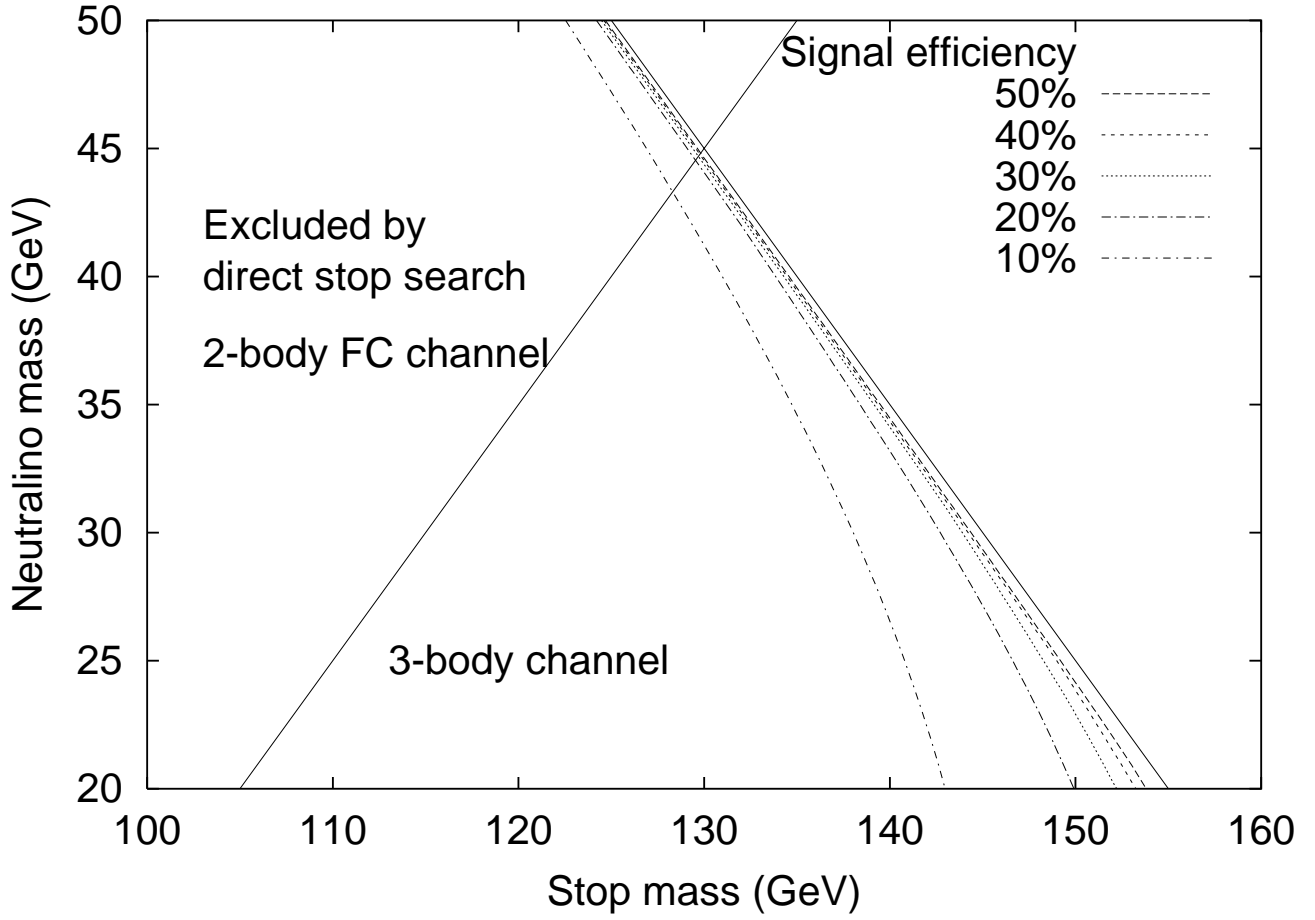


Figure 6: 5σ discovery contours for top quark decays to stops at Run II with 4 fb^{-1} for various signal efficiencies, in the case that $\tilde{t}_1 = \tilde{t}_L$, which gives the smallest event rates. The case $\tilde{t}_1 = \tilde{t}_R$ would be discovered virtually up to the kinematic limit even with 10% signal efficiency, and is not shown here. The solid lines are as in Fig. 5.

is considerably higher. This allows top quark decays to $\tilde{t}\tilde{\chi}_1^0$ to be detected for stop and neutralino masses above the Run I bound. For $\tilde{t}_1 = \tilde{t}_R$, top quark decays to stops will be probed virtually up to the kinematic limit, even with low signal efficiency $\sim 10\%$ and only 2 fb^{-1} of integrated luminosity. If $\tilde{t}_1 = \tilde{t}_L$, so that the signal event rate is minimized, top quark decays to stops would be discovered up to within 10 GeV of the kinematic limit for signal efficiencies $\gtrsim 20\%$ and 4 fb^{-1} of integrated luminosity (see Fig. 6). In this region of parameter space, stops would also be discovered in Run II with less than 2 fb^{-1} via direct stop pair production (see Fig. 4).

6 Ten degenerate squarks

Having concentrated until now on the production and decay of the top squark, let us now consider the other squarks. In the most general MSSM, the spectrum is of course quite arbitrary. However, low energy constraints [32] from flavor changing neutral current processes demand that such squarks be nearly mass degenerate, at least those of the same chirality. Interestingly, in many theoretical scenarios, such as the minimal gauge mediated models, this mass degeneracy between squarks of the same chirality happens naturally; in addition the mass splitting between the left-handed and right-handed squarks associated with the five light quarks turns out to be small. For simplicity, then, we will work under the approximation that all of these 10 squarks (namely, $\tilde{u}_{L,R}$, $\tilde{d}_{L,R}$, $\tilde{c}_{L,R}$, $\tilde{s}_{L,R}$ and $\tilde{b}_{L,R}$) are exactly degenerate.

6.1 Production at Tevatron Run II

While the cross sections for the individual pair-production of the $\tilde{c}_{L,R}$, $\tilde{s}_{L,R}$ and $\tilde{b}_{L,R}$ are essentially the same as that for a top-squark of the same mass, the situation is more complicated for squarks of the first generation. The latter depend sensitively on the gluino mass because of the presence of t -channel diagrams. Moreover, processes such as $\bar{u}u \rightarrow \tilde{u}_L \tilde{u}_R^*$ or $dd \rightarrow \tilde{d}_{L,R} \tilde{d}_{L,R}$ become possible and relevant. Of course, in the limit of very large gluino mass, the squark production processes are driven essentially by QCD and dominated by the production of pairs of mass eigenstates, analogous to the top squark production considered already. In particular, at the leading order, the total production cross section for the ten degenerate squarks of a given mass is simply ten times the corresponding top squark production cross section.

Since a relatively light gluino only serves to increase the total cross section (see Fig. 7), it can be argued that the heavy gluino limit is a *conservative one*. To avoid considering an additional free parameter, we shall perform our analysis in this limit. To a first approximation, the signal cross sections presented below will scale¹⁷ with the gluino mass approximately as shown in Fig. 7.

Like top squarks, the 10 degenerate squarks can also be produced via cascade decays of heavier supersymmetric particles. To be conservative, we again neglect this source of squark production by assuming that the masses of the heavier supersymmetric particles are large enough that their production rate at Tevatron energies can be neglected.

The NLO cross sections for production of ten degenerate squarks including QCD and SUSY-QCD corrections have been implemented numerically in PROSPINO [18]. We generate squark production events using the LO cross section evaluated at the scale $\mu = m_{\tilde{q}}$, improved by the NLO K-factor obtained from

¹⁷That the gluino exchange diagram has a different topology as compared to the (dominant) quark-initiated QCD diagram indicates that corresponding angular distributions would be somewhat different. Thus, the efficiency after cuts is not expected to be strictly independent of the gluino mass. For the most part, though, this is only a subleading effect.

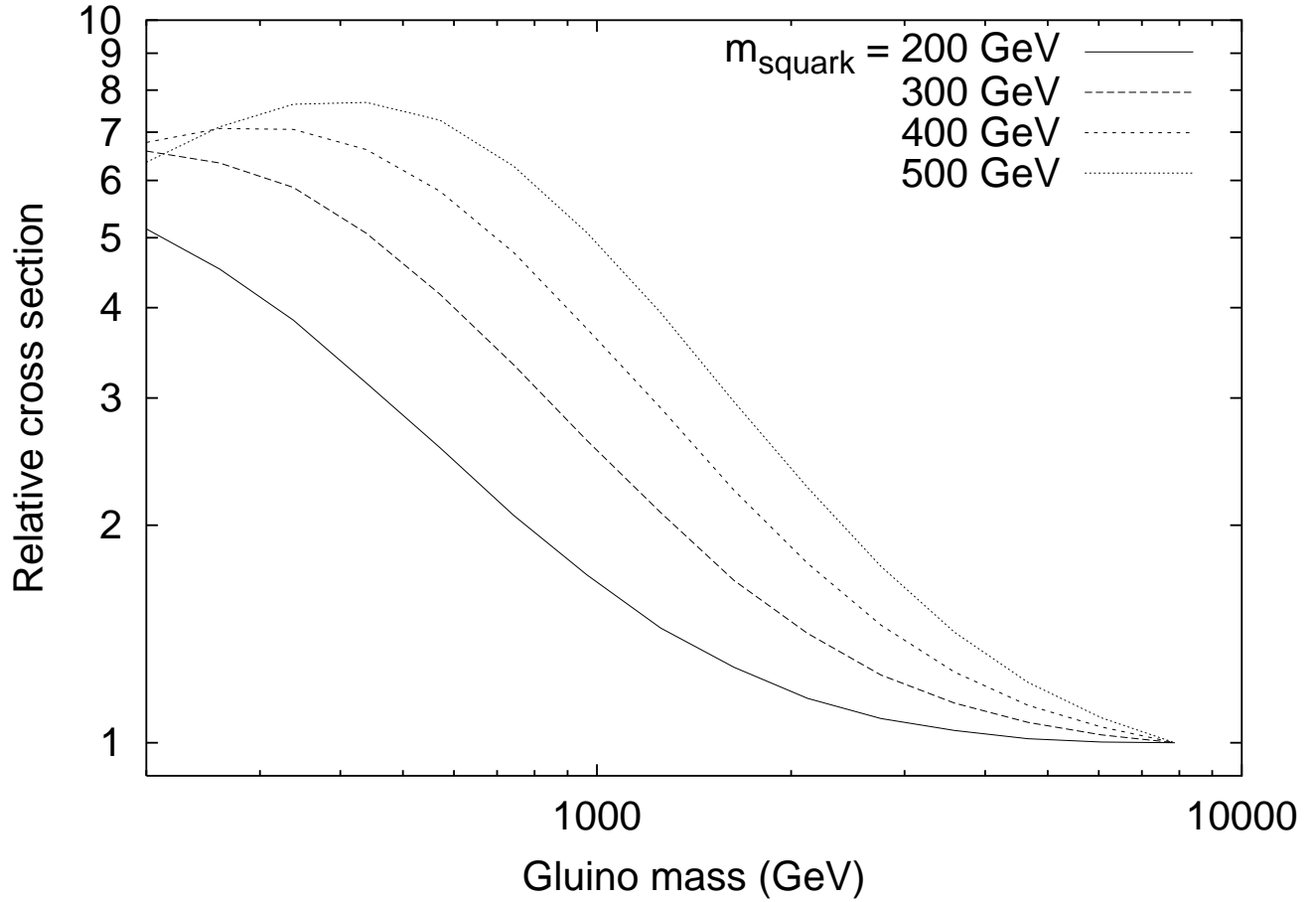


Figure 7: Gluino mass dependence of the NLO cross section for production of ten degenerate squarks in 2 TeV $p\bar{p}$ collisions, from PROSPINO [18]. Shown are the cross sections for $\tilde{q}\tilde{q}^*$ production normalized to the value at large $m_{\tilde{g}}$, for common squark masses of 200, 300, 400 and 500 GeV. Production of $\tilde{q}\tilde{q}$ is small at a $p\bar{p}$ collider and is neglected here; it yields an additional 3-15% increase in the total cross section at low $m_{\tilde{g}}$ for this range of squark masses. Cross sections are evaluated at the scale $\mu = m_{\tilde{q}}$.

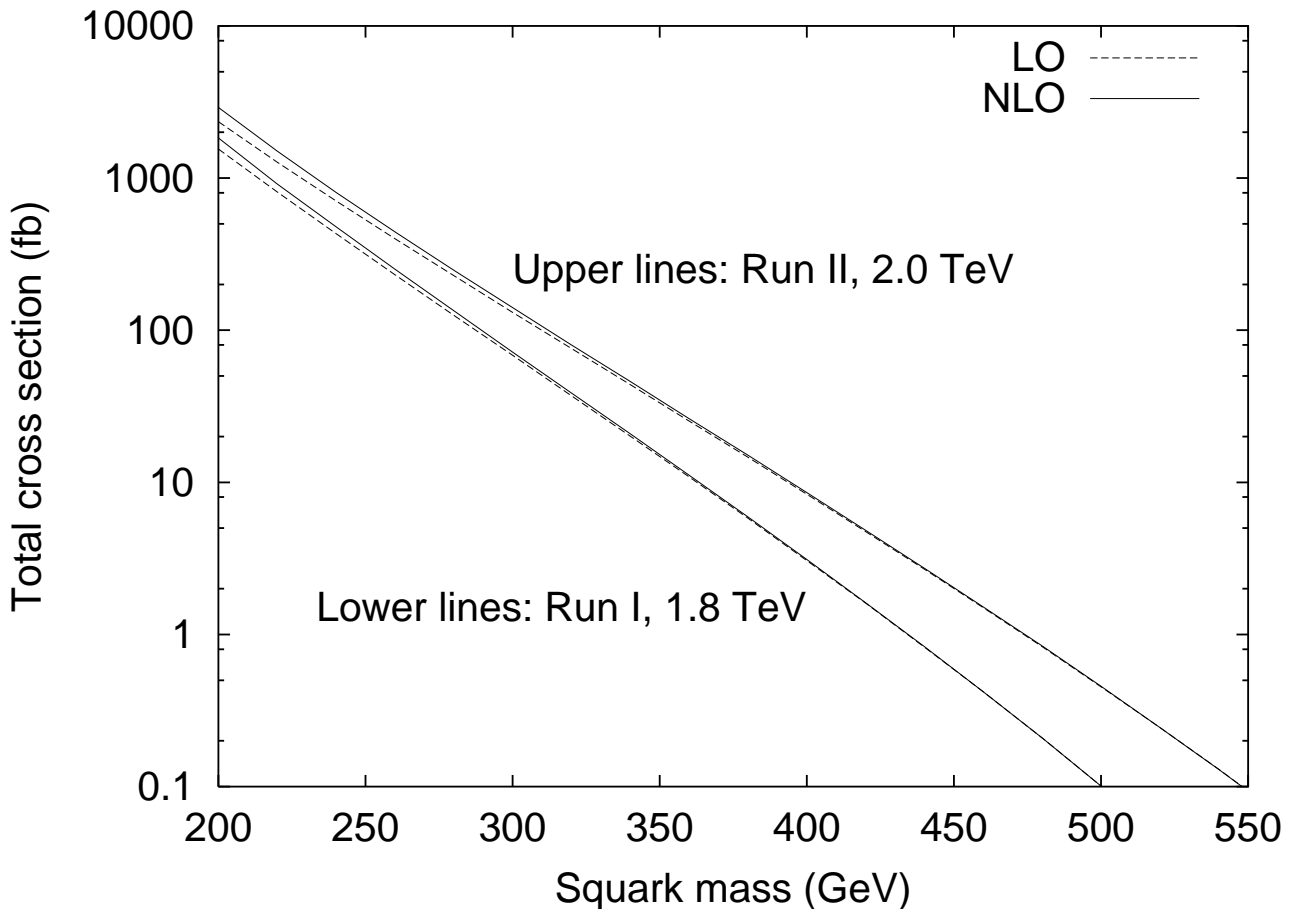


Figure 8: LO and NLO cross section for the production of ten degenerate squarks in the heavy gluino limit in $p\bar{p}$ collisions at Tevatron Run I (1.8 TeV) and Run II (2.0 TeV), from PROSPINO [18]. Cross sections are evaluated at the scale $\mu = m_{\tilde{q}}$.

PROSPINO [18] (see Fig. 8), in the limit that the gluino is very heavy. The K-factor varies between 1 and 1.25 for $m_{\tilde{q}}$ decreasing from 550 to 200 GeV. As in the case of the top squark analysis, we use the CTEQ5 parton distribution functions [19] and neglect the shift in the p_T distribution of the squarks due to gluon radiation at NLO.

6.2 Signals in low-energy SUSY breaking

The decays of the ten degenerate squarks are very simple. As long as they are heavier than the lightest neutralino,¹⁸ they decay via $\tilde{q} \rightarrow q\tilde{\chi}_1^0 \rightarrow q\gamma\tilde{G}$. The signal and backgrounds are then identical to those of the two-body FC stop decay discussed in Sec. 5.1, and consequently we use the same selection cuts. In fact, in view of the tenfold increase in the signal strength, we could afford more stringent cuts so as to

¹⁸As before, we do not allow the possibility of cascade decays through other neutralinos/charginos. Were we to allow these, the channel we are considering would be somewhat suppressed, but additional, more spectacular, channels would open up.

eliminate virtually all backgrounds, but this is not quite necessary.

The signal cross section after cuts (but before efficiencies) for production of ten degenerate squarks in the heavy gluino limit is shown in Fig. 9 as contours in the $m_{\tilde{q}}-m_{\tilde{\chi}_1^0}$ plane. We assume that the squark \tilde{q} decays predominantly into $q\tilde{\chi}_1^0$. The branching ratio of $\tilde{\chi}_1^0 \rightarrow \gamma\tilde{G}$ is taken from Fig. 2 assuming that $\tilde{\chi}_1^0$ is a pure bino. Clearly, the effect of the kinematic cuts on the signal is very similar to that in the case of the 2-body FC decay of the stop. The mass reach, of course, is much larger due to the tenfold increase in the total cross section; also, unlike in the case of the stop, the 2-body decay is dominant throughout the entire parameter space.

The non-observation of $jj\gamma\gamma\not{E}_T$ events at Run I of the Tevatron excludes the region of parameter space shown in black in Fig. 9. As in our stop analysis, in this excluded region, at least 3 signal events would have been detected in the 100 pb^{-1} of Run I data, with negligible background. In particular, we estimate that Run I data excludes the ten degenerate squarks up to a common mass of about 280 GeV. As in the case of 2-body FC stop decays, when the mass splitting between the squarks and the neutralino is too small (*i.e.*, less than about 40 GeV), the jets become soft and the signal efficiency decreases dramatically, leaving an unexcluded region of parameter space. The $D\bar{O}$ search for inclusive $p\bar{p} \rightarrow \tilde{\chi}_2^0 + X$ with $\tilde{\chi}_2^0 \rightarrow \gamma\tilde{\chi}_1^0$ [28] yields a limit on the production cross section of about 0.5 pb for parent squark masses above about 250 GeV. Interpreted in terms of pair production of 10 degenerate squarks in the large $m_{\tilde{g}}$ limit with $\tilde{\chi}_2^0 \rightarrow \gamma\tilde{\chi}_1^0$ reidentified as $\tilde{\chi}_1^0 \rightarrow \gamma\tilde{G}$ again increases the signal efficiency by a factor of ~ 2.7 because every event contains two photons [28]; the $D\bar{O}$ analysis then yields a bound on the common squark mass of about 275 GeV, again in rough agreement with our result.¹⁹

Taking the total background cross section to be 2 fb (see Table 1), we show in Table 5 the expected maximum discovery mass reach for ten degenerate squarks at Tevatron Run II for various amounts of integrated luminosity.²⁰ In particular, with 4 fb^{-1} a squark discovery can be expected in this channel if $m_{\tilde{q}} < 360$ GeV. Again, if the lightest neutralino is not a pure bino, the reach at large neutralino masses will be reduced. However, this will have very little effect on the maximum squark mass reach quoted here, because this maximum reach occurs for $m_{\tilde{\chi}_1^0} \sim 100 - 150$ GeV, where all neutralino decay modes other than $\gamma\tilde{G}$ suffer a large kinematic suppression. From Fig. 2, it is evident that the neutralino branching fraction into $\gamma\tilde{G}$ will be reduced by no more than 10% in this mass range as long as the neutralino is at least 50% bino; such a reduction in the neutralino branching fraction will lead to a reduction of only a few GeV in the maximum squark mass reach.

¹⁹Ref. [28] quotes a squark mass bound of 320 GeV for the case $m_{\tilde{q}} \ll m_{\tilde{g}}$ in the context of low-energy SUSY breaking; we expect that this is due to the contribution of chargino and neutralino production to the total SUSY cross section in their analysis.

²⁰Again, if data from the CDF and $D\bar{O}$ detectors are combined, the integrated luminosity of the machine is effectively doubled.

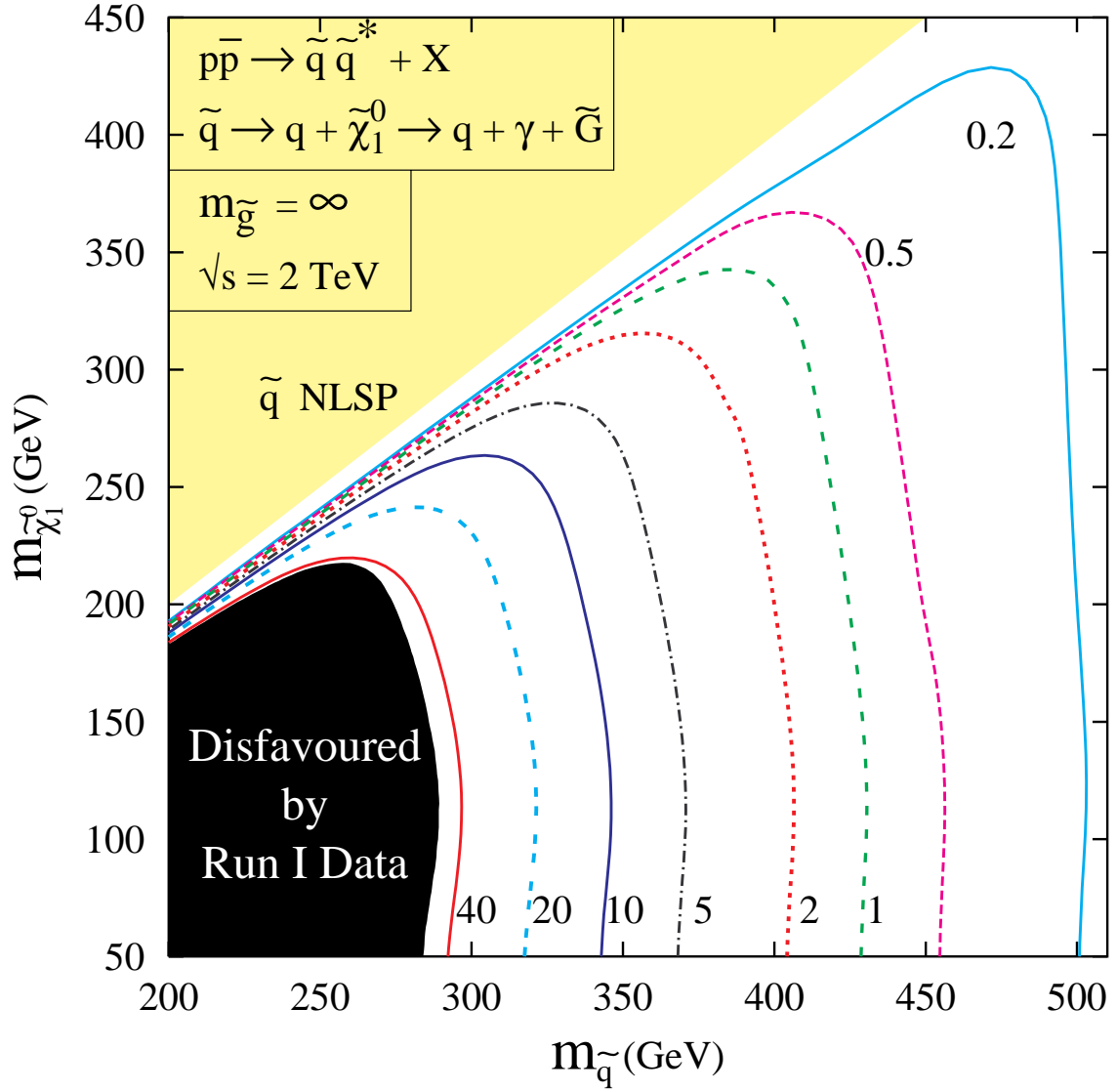


Figure 9: Cross section in fb for production of 10 degenerate squarks in Run II in the heavy gluino limit with $\tilde{q} \rightarrow q\gamma\tilde{G}$, after cuts. The black area is excluded by non-observation of $jj\gamma\gamma\cancel{E}_T$ events in Run I.

$\int \mathcal{L}$	B	S for a 5σ discovery	$\sigma_S \times \epsilon_\gamma^2$	Maximum squark mass reach
2 fb^{-1}	4	14	7.0 fb	345 GeV
4 fb^{-1}	8	18	4.5 fb	360 GeV
15 fb^{-1}	30	31	2.1 fb	390 GeV
30 fb^{-1}	60	42	1.4 fb	405 GeV

Table 5: Number of signal events (S) required for a 5σ squark discovery at Tevatron Run II, assuming production of 10 degenerate squarks in the limit that the gluino is very heavy, and the corresponding signal cross section after cuts and efficiencies and maximum squark mass reach. We take $\epsilon_\gamma = 0.80$. The number of background events (B) is based on a background cross section of 2 fb from Table 1.

7 Conclusions

In models of low-energy SUSY breaking, signatures of SUSY particle production generically contain two hard photons plus missing energy due to the decays of the two neutralino NLSPs produced in the decay chains. Standard Model backgrounds to such signals are naturally small at Run II of the Tevatron. We studied the production and decay of top squarks at the Tevatron in such models in the case where the lightest Standard Model superpartner is a light neutralino that predominantly decays into a photon and a light gravitino. We considered 2-body flavor-changing and 3-body decays of the top squarks. The reach of the Tevatron in such models is larger than in the standard supergravity models and than in models with low-energy SUSY breaking in which the stop is the NLSP, rather than the neutralino. We estimate that top squarks with masses below about 200 GeV can be excluded based on Run I data, assuming that $50 \text{ GeV} \lesssim m_{\tilde{\chi}_1^0} \lesssim m_{\tilde{t}} - 10 \text{ GeV}$. For a modest final Run II luminosity of 4 fb^{-1} , stop masses up to 285 GeV are accessible in the 2-body decay mode, and up to 320 GeV in the 3-body decay mode.

Top squarks can also be produced in top quark decays. We found that, within the context of low-energy SUSY breaking with the stop as the next-to-next-to-lightest SUSY particle, the region of parameter space in which stop production in top quark decays is possible is almost entirely excluded by Run I data if the lighter stop is predominantly right handed; however, an interesting region is still allowed if the lighter stop is predominantly left handed, due to the smaller branching ratio of $t \rightarrow \tilde{t}_L \tilde{\chi}_1^0$. Run II will cover the entire parameter space in which top decays to stop are possible.

We also studied the production and decay of the ten squarks associated with the five light quarks, assumed to be degenerate. In models of low-energy SUSY breaking, the decays of the ten degenerate squarks lead to signals identical to those for the 2-body flavor-changing stop decays. The cross section for production of ten degenerate squarks at the Tevatron is significantly larger than that of the top squark. We estimate that the 10 degenerate squarks with masses below about 280 GeV can be excluded based on

Run I data, assuming that $m_{\tilde{\chi}_1^0} \lesssim m_{\tilde{q}} - 40$ GeV. For a final Run II luminosity of 4 fb^{-1} , squark masses as large as 360 GeV are easily accessible in the limit that the gluino is very heavy. The production cross section, and hence the discovery reach, increases further with decreasing gluino mass.

Acknowledgments

We are very grateful to Michael Schmitt for helping us understand instrumental backgrounds and detector capabilities. We also thank Ray Culbertson, Joel Goldstein, Tilman Plehn, and David Rainwater for useful discussions. Fermilab is operated by Universities Research Association Inc. under contract no. DE-AC02-76CH03000 with the U.S. Department of Energy. D.C. thanks the Theory Division of Fermilab for hospitality while part of the project was being carried out and the Deptt. of Science and Technology, India for financial assistance under the Swarnajayanti Fellowship grant. R.A.D. thanks Fermilab for its kind hospitality and financial support and DINAIN (Colombia) for financial support. C.W. is supported in part by the US DOE, Division of High-Energy Physics, under contract no. W-31-109-ENG-38.

References

- [1] H. E. Haber and G. L. Kane, Phys. Rept. **117**, 75 (1985); H. P. Nilles, Phys. Rept. **110**, 1 (1984).
- [2] M. Carena, J. R. Espinosa, M. Quiros and C. E. Wagner, Phys. Lett. B **355**, 209 (1995); M. Carena, M. Quiros and C. E. Wagner, Nucl. Phys. B **461**, 407 (1996); H. E. Haber, R. Hempfling and A. H. Hoang, Z. Phys. C **75**, 539 (1997); R. J. Zhang, Phys. Lett. B **447**, 89 (1999); J. R. Espinosa and R. J. Zhang, Nucl. Phys. B **586**, 3 (2000); A. Brignole, G. Degrassi, P. Slavich and F. Zwirner, Nucl. Phys. B **631**, 195 (2002); S. Heinemeyer, W. Hollik and G. Weiglein, Phys. Rev. D **58**, 091701 (1998); Phys. Lett. B **440**, 296 (1998); Eur. Phys. J. C **9**, 343 (1999).
- [3] P. Fayet, Phys. Lett. B **70**, 461 (1977); B **86**, 272 (1979); B **175**, 471 (1986).
- [4] M. Dine, W. Fischler, and M. Srednicki, Nucl. Phys. B **189**, 575 (1981); S. Dimopoulos and S. Raby, Nucl. Phys. B **192**, 353 (1981); M. Dine and W. Fischler, Phys. Lett. B **110**, 227 (1982); Nucl. Phys. B **204**, 346 (1982); M. Dine and M. Srednicki, Nucl. Phys. B **202**, 238 (1982); L. Alvarez-Gaumé, M. Claudson, and M. Wise, Nucl. Phys. B **207**, 96 (1982); C.R. Nappi and B.A. Ovrut, Phys. Lett. B **113**, 175 (1982); S. Dimopoulos and S. Raby, Nucl. Phys. B **219**, 479 (1983).
- [5] M. Dine and A.E. Nelson, Phys. Rev. D **48**, 1277 (1993); M. Dine, A. E. Nelson and Y. Shirman, Phys. Rev. D **51**, 1362 (1995); M. Dine, A. E. Nelson, Y. Nir and Y. Shirman, Phys. Rev. D **53**, 2658 (1996).

- [6] M. Carena, S. Pokorski and C. E. Wagner, *Phys. Lett. B* **430**, 281 (1998).
- [7] R. Culbertson *et al.*, “Low-scale and gauge-mediated supersymmetry breaking at the Fermilab Tevatron Run II”, arXiv:hep-ph/0008070.
- [8] S. Dimopoulos, M. Dine, S. Raby and S. Thomas, *Phys. Rev. Lett.* **76**, 3494 (1996). S. Dimopoulos, S. Thomas and J. D. Wells, *Nucl. Phys. B* **488**, 39 (1997).
- [9] S. Ambrosanio, G. L. Kane, G. D. Kribs, S. P. Martin and S. Mrenna, *Phys. Rev. D* **54**, 5395 (1996).
- [10] A. Brignole, F. Feruglio, M. L. Mangano and F. Zwirner, *Nucl. Phys. B* **526**, 136 (1998) [Erratum *Nucl. Phys. B* **582**, 759 (2000)]; E. Perazzi, G. Ridolfi and F. Zwirner, *Nucl. Phys. B* **590**, 287 (2000).
- [11] H. Komatsu and J. Kubo, *Phys. Lett. B* **157**, 90 (1985); M. Quiros, G. Kane and H.E. Haber, *Nucl. Phys. B* **273**, 333 (1996); H.E. Haber and D. Wyler, *Nucl. Phys. B* **323**, 267 (1989); S. Ambrosanio and B. Mele, *Phys. Rev. D* **55**, 1399 (1997) [Erratum *Phys. Rev. D* **56**, 3157 (1997)].
- [12] S. Ambrosanio, G.L. Kane, G.D. Kribs, and S.P. Martin, *Phys. Rev. Lett.* **76**, 3498 (1996).
- [13] See, for example, <http://lepsusy.web.cern.ch/lepsusy/>
- [14] M. Carena, M. Quiros and C.E.M. Wagner, *Phys. Lett. B* **380**, 81 (1996); D. Delepine, J.M. Gérard, R. González Felipe and J. Weyers, *Phys. Lett. B* **386**, 183 (1996); J. Cline and K. Kainulainen, *Nucl. Phys. B* **482**, 73 (1996); *Nucl. Phys. B* **510**, 88 (1998); J.R. Espinosa, *Nucl. Phys. B* **475**, 273 (1996); B. de Carlos and J.R. Espinosa, *Nucl. Phys. B* **503**, 24 (1997); D. Bodeker, P. John, M. Laine and M.G. Schmidt, *Nucl. Phys. B* **497**, 387 (1997); M. Carena, M. Quiros and C.E.M. Wagner, *Nucl. Phys. B* **524**, 3 (1998); M. Laine and K. Rummukainen, *Nucl. Phys. B* **535**, 423 (1998); F. Csikor, Z. Fodor, P. Hegedus, A. Jakovac, S.D. Katz and A. Piroth, *Phys. Rev. Lett.* **85**, 932 (2000); M. Losada, *Nucl. Phys. B* **537**, 3 (1999); *Nucl. Phys. B* **569**, 125 (2000).
- [15] P. R. Harrison and C. H. Llewellyn Smith, *Nucl. Phys. B* **213**, 223 (1983) [Erratum *B* **223**, 542 (1983)].
- [16] S. Dawson, E. Eichten and C. Quigg, *Phys. Rev. D* **31**, 1581 (1985).
- [17] W. Beenakker, M. Kramer, T. Plehn, M. Spira and P. M. Zerwas, *Nucl. Phys. B* **515**, 3 (1998).
- [18] W. Beenakker, R. Hopker and M. Spira, arXiv:hep-ph/9611232.
- [19] H. L. Lai *et al.* [CTEQ Collaboration], *Eur. Phys. J. C* **12**, 375 (2000).
- [20] R. Demina, J. D. Lykken, K. T. Matchev and A. Nomerotski, *Phys. Rev. D* **62**, 035011 (2000).
- [21] A. Mafi and S. Raby, *Phys. Rev. D* **62**, 035003 (2000)

- [22] M. Carena, S. Heinemeyer, C. E. Wagner and G. Weiglein, *Phys. Rev. Lett.* **86**, 4463 (2001); E. L. Berger, B. W. Harris, D. E. Kaplan, Z. Sullivan, T. M. Tait and C. E. Wagner, *Phys. Rev. Lett.* **86**, 4231 (2001).
- [23] C. L. Chou and M. E. Peskin, *Phys. Rev. D* **61**, 055004 (2000).
- [24] S. P. Das, A. Datta and M. Guchait, arXiv:hep-ph/0112182.
- [25] T. Stelzer and W. F. Long, *Comput. Phys. Commun.* **81**, 357 (1994).
- [26] T. Affolder *et al.* [CDF Collaboration], *Phys. Rev. D* **65**, 052006 (2002).
- [27] F. Abe *et al.* [CDF Collaboration], *Phys. Rev. Lett.* **77**, 2616 (1996); T. Affolder *et al.* [CDF Collaboration], *Phys. Rev. Lett.* **87**, 131802 (2001).
- [28] B. Abbot *et al.* [D0 Collaboration], *Phys. Rev. Lett.* **82**, 29 (1998).
- [29] W. Porod, Ph.D. thesis, arXiv:hep-ph/9804208.
- [30] See, *e.g.*, E. L. Berger and H. Contopanagos, *Phys. Rev. D* **54**, 3085 (1996); S. Catani, M. L. Mangano, P. Nason and L. Trentadue, *Phys. Lett. B* **378**, 329 (1996); N. Kidonakis, *Phys. Rev. D* **64**, 014009 (2001); N. Kidonakis, hep-ph/0110145 and references therein.
- [31] B. Abbot *et al.* [D0 Collaboration], *Phys. Rev. Lett.* **80**, 442 (1998).
- [32] J. R. Ellis and D. V. Nanopoulos, *Phys. Lett. B* **110**, 44 (1982); F. Gabbiani and A. Masiero, *Nucl. Phys. B* **322**, 235 (1989); S. Bertolini, F. Borzumati, A. Masiero and G. Ridolfi, *Nucl. Phys. B* **353**, 591 (1991); J. S. Hagelin, S. Kelley and T. Tanaka, *Nucl. Phys. B* **415**, 293 (1994); D. Choudhury, F. Eberlein, A. Konig, J. Louis and S. Pokorski, *Phys. Lett. B* **342**, 180 (1995); M. Ciuchini *et al.*, *JHEP* **9810**, 008 (1998).